Geochemistry and petrology of mafic Proterozoic and Permian dykes on Bornholm, Denmark: Four episodes of magmatism on the margin of the Baltic Shield

P.M. HOLM, L.E. PEDERSEN & B. HØJSTEEN

Holm, P.M., Pedersen, L.E. & Højsteen, B., 2010–05–17. Geochemistry and petrology of mafic Proterozoic and Permian dykes on Bornholm, Denmark: Four episodes of magmatism on the margin of the Baltic Shield. © 2010 by Bulletin of the Geological Society of Denmark, Vol. 58, pp. 35–65. ISSN 0011–6297. (www.2dgf.dk/publikationer/bulletin) https://doi.org/10.37570/bgsd-2010-58-04

More than 250 dykes cut the mid Proterozoic basement gneisses and granites of Bornholm. Most trend between NNW and NNE, whereas a few trend NE and NW. Field, geochemical and petrological evidence suggest that the dyke intrusions occurred as four distinct events at around 1326 Ma (Kelseaa dyke), 1220 Ma (narrow dykes), 950 Ma (Kaas and Listed dykes), and 300 Ma (NW-trending dykes), respectively.

The largest dyke at Kelseaa (60 m wide) and some related dykes are primitive olivine tholeiites, one of which has N-type MORB geochemical features; all are crustally contaminated. The Kelseaa type magmas were derived at shallow depth from a fluid-enriched, relatively depleted, mantle source, but some have a component derived from mantle with residual garnet. They are suggested to have formed in a back-arc environment.

The more than 200 narrow dykes are olivine tholeiites (some picritic), alkali basalts, trachybasalts, basanites and a few phonotephrites. The magmas evolved by olivine and olivine + clinopyroxene fractionation. They have trace element characteristics which can be described mainly by mixing of two components: one is a typical OIB-magma (La/Nb < 1, Zr/Nb = 4, Sr/Nd = 16) and rather shallowly derived from spinel peridotite; the other is enriched in Sr and has La/Nb = 1.0 - 1.5, Zr/Nb = 9, Sr/Nd = 30 and was derived at greater depth, probably from a pyroxenitic source. Both sources were probably recycled material in a mantle plume. A few of these dykes are much more enriched in incompatible elements and were derived from garnet peridotite by a small degree of partial melting. The Kaas and Listed dykes (20-40 m) and related dykes are evolved trachybasalts to basaltic trachyandesites. They are most likely related to the Blekinge Dalarne Dolerite Group. The few NW-trending dykes are quartz tholeiites, which were generated by large degrees of rather shallow melting of an enriched mantle source more enriched than the source of the older Bornholm dykes. The source of the NW-trending dykes was probably a very hot mantle plume.

Keywords: Bornholm, dykes, Baltic Shield, petrology, geochemistry.

Paul Martin Holm [paulmh@geo.ku.dk], Department of Geography and Geology, University of Copenhagen, Øster Voldgade 10, DK-1350 Copenhagen K.

Geological setting

The Baltic Shield is separated from the Danish-Polish Basin by two major fault zones, the Sorgenfrei-Tornquist zone (STZ) and the Teisseyre-Tornquist zone (TTZ) (Fig.1). Bornholm island is situated just E of the Rønne Graben, which offsets the STZ and TTZ. The southern part of the island is covered by Phanerozoic sediments, while Proterozoic basement rocks are exposed in the northern part. The geology of Bornholm has been described by e.g. Callisen (1934), Münther (1973), Micheelsen (1961), Surlyk (1980) and Berthelsen (1989, 1992).

The basement gneisses of Bornholm have been considered to belong to the same province as the coastal gneisses in Blekinge (Sweden) north of Bornholm (Berthelsen, 1989). The latter were formed probably as juvenile crust in Gothian times around 1.8 – 1.7 Ga (Johansson & Larsen, 1989; Johansson et al., 2006). The gneisses are intruded by two generations of granites. The older granites have gradational contacts to the gneisses (Callisen, 1934), and Berthelsen (1989)

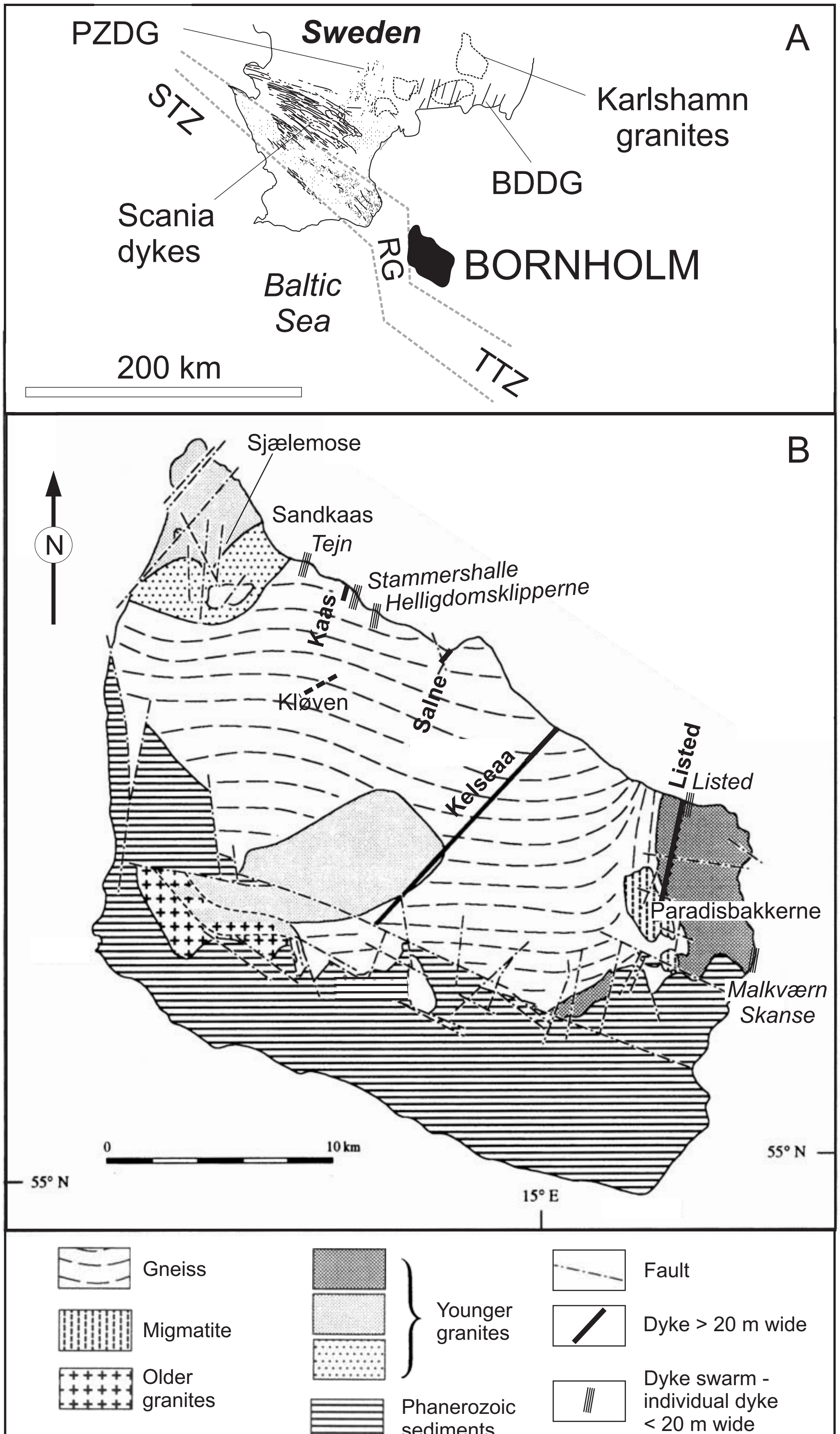

Figure 1: A: The location of Bornholm on the margin of the Baltic Shield. Also shown are three Swedish dyke swarms (PZDG – Protogine Zone Dolerite Group trending NNE, BDDG – Blekinge Dalarne Dolerite Group, Scania dykes), the Karlshamn granites, the Sorgenfrei-Tornquist Zone – STZ, the Teisseyre-Tornquist Zone – TTZ, and the Rønne Graben - RG. B: Geological map of Bornholm showing schematically the locations of large dykes (in bold) and dyke swarms (in italics). The geological map, apart from the dykes, is after Platou (1970). Modified from Abrahamsen & Lewandowski (1995). The authors have retained old spelling of place names related to dykes mentioned in the litterature. New spelling of Keldseaa is Kelse Å, Kaas is now Kås, and Strandkaas is Strandkås

suggested an origin by partial melting of the gneisses. The older granites are deformed. A younger generation of undeformed granites has sharp intrusive contacts to the gneisses. The granites were dated by Rb-Sr (Larsen, 1980) to 1400 ± 60 Ma (2σ) and subsequently by U-Pb (Tschernoster, 2000, Čečys, 2004). Recently, a much more restricted age range has been argued for the Bornholm gneisses and granites as more precise U-Pb analyses of zircon and titanite indicate that all granites crystallized in the interval 1475 - 1445 Ma, and that the orthogneiss country rocks have similar crystallization ages (Zariņš & Johansson, 2008). Gothian crust seems to be present only as inherited zircons in the gneisses (Zariņš & Johansson, 2008). The gneisses of Bornholm are therefore not equivalent to those of Blekinge which are Gothian with an age of 1.8 Ga (Johansson et al., 2006).

The deformation and granitic magmatism at c. 1.45 Ga is contemporaneous with similar events in Blekinge and elsewhere along the southwest margin of Baltica (Åberg, 1988; Obst et al., 2004; Johansson et al., 2006; Čečys & Benn, 2007; Bogdanova et al., 2008), which were termed the "Danopolonian orogeny" by Bogdanova (2001).

Extensional events in SW Sweden at around 1.2 Ga were accompanied by dyke intrusions at and parallel to the NNE-trending Protogine Zone (Fig. 1), and were correlated with a possible back-arc setting prior to the Sweconorwegian orogeny (Söderlund et al., 2005; Söderlund & Ask, 2006).

The Bornholm dykes

More than 250 mafic dykes have been intruded into the gneissic and granitic basement of Bornholm (Fig. 2), and their distribution and petrography have been described by Callisen (1934) and Münther (1945a, 1945b). Jensen (1966, 1988) has presented detailed petrography for a few selected dykes, and Obst (2000) discusses the petrology of the WNW- to NW-trending dykes. Abrahamsen (1977) and Abrahamsen & Lewandowski (1995) investigated the paleomagnetism of a wide range of dykes.

The dykes are mainly exposed along the north coast which is oblique to the trend of the dykes (Figs. 3 & 4a). The mafic dykes are estimated to have caused a minimum of 1.3% dilation along the c. 30 km long coast (Münther, 1945a, 1973). Almost all dykes strike between NNE and NNW (Fig. 4) and all are near-vertical. Among the exceptions are the Kelseaa dyke which strikes 40°, and a few WNW- to NW-striking dykes (Forchhammer, 1847; Münther, 1945b). Dykes exposed in inland areas and along the east and west coasts have similar orientations to the majority of dykes along the north coast. The width distribution of the dykes is strongly bimodal, in the sense that four dykes are 20 to 60 metres wide, whereas most of them are only a few metres wide (86 % are less than 3 m wide).

The Kelseaa dyke is the largest with a width of 60 m; it can be traced along strike for c. 20 km by detailed magnetic (Münther, 1973) and gravity measurements (Saxov, 1958). It is a significant gabbroic intrusion with an exposed area of almost 1.5 km^2. The Kaas dyke is

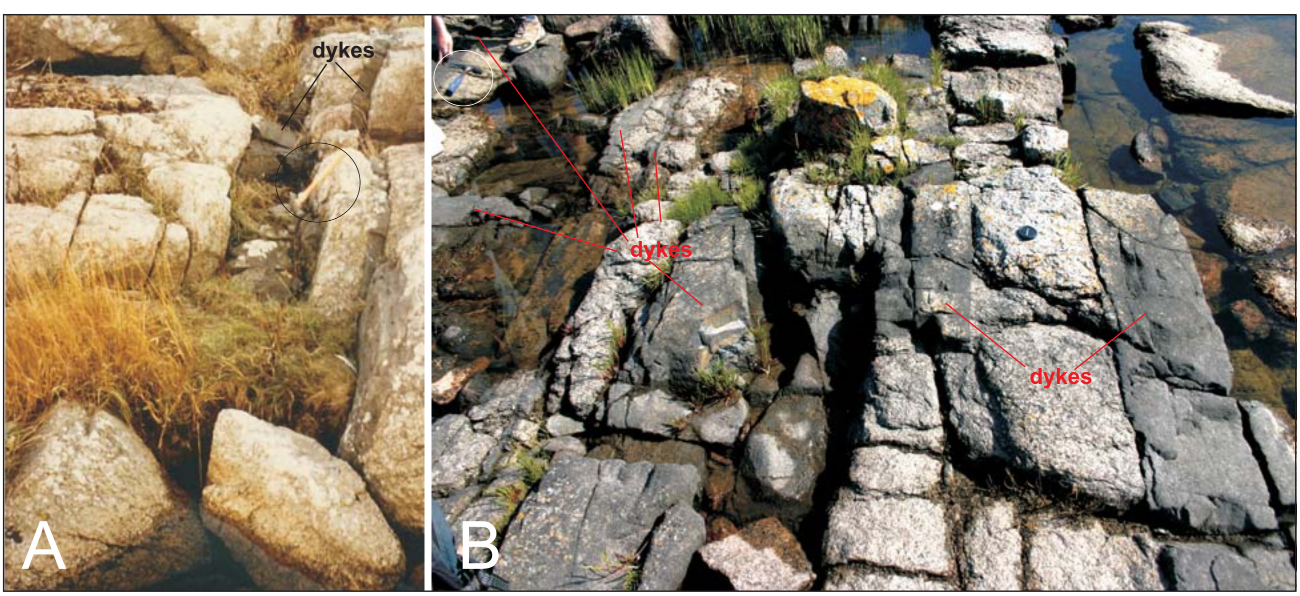

Figure 2: A) NNE-trending basaltic dykes cutting gneiss on the north coast of Bornholm. B) Part of the NNE-trending swarm on the east coast of Bornholm at Malkværn Skanse (hammer for scale in both photographs is 30 cm long) cutting the Svaneke granite.

40 m wide, but is exposed only over a short distance from the coast, whereas the 30 m wide Listed dyke can be traced 5 km inland. The Salne dyke is 22 m wide. Münther (1945a) lists four dyke swarms (Figs 3, 5): east of Tejn harbour where dykes make up around 20 % of the exposure over 150 m along the coast (Fig. 3A); around Stammershalle where > 16 dykes make up 7 % of the area for 300 m (Fig. 3B); in the Helligdomsklipperne area with 5 % dykes over 600 m of coast (Fig. 3C); and from east of Listed harbour to near the mouth of Vaseå stream dykes constitute c. 10 % of the crust over 550 m of coast line (Fig. 3G). However, the latter swarm includes the large dyke at Listed, which makes up 30 m of the 46.5 m total dyke width. The Listed dyke may be considerably younger than the other dykes (see below), which makes the concentration of the other, possibly penecontemporaneous, dykes in the area much lower (3.5 %) and they would probably not be considered to represent a swarm on their own. The easternmost dykes around Malkværn Skanse (Figs. 3H & 5b), on the other hand, constitute 7 % of the crust over a distance of 250 m in an ENE direction, and should therefore be considered a swarm. The term "dyke swarm" is used here for local concentrations that on Bornholm never represent more than 20 % crustal dilation. WNW- to NW-trending dykes are rare and constitute a relatively minor component of the mafic intrusions on Bornholm.

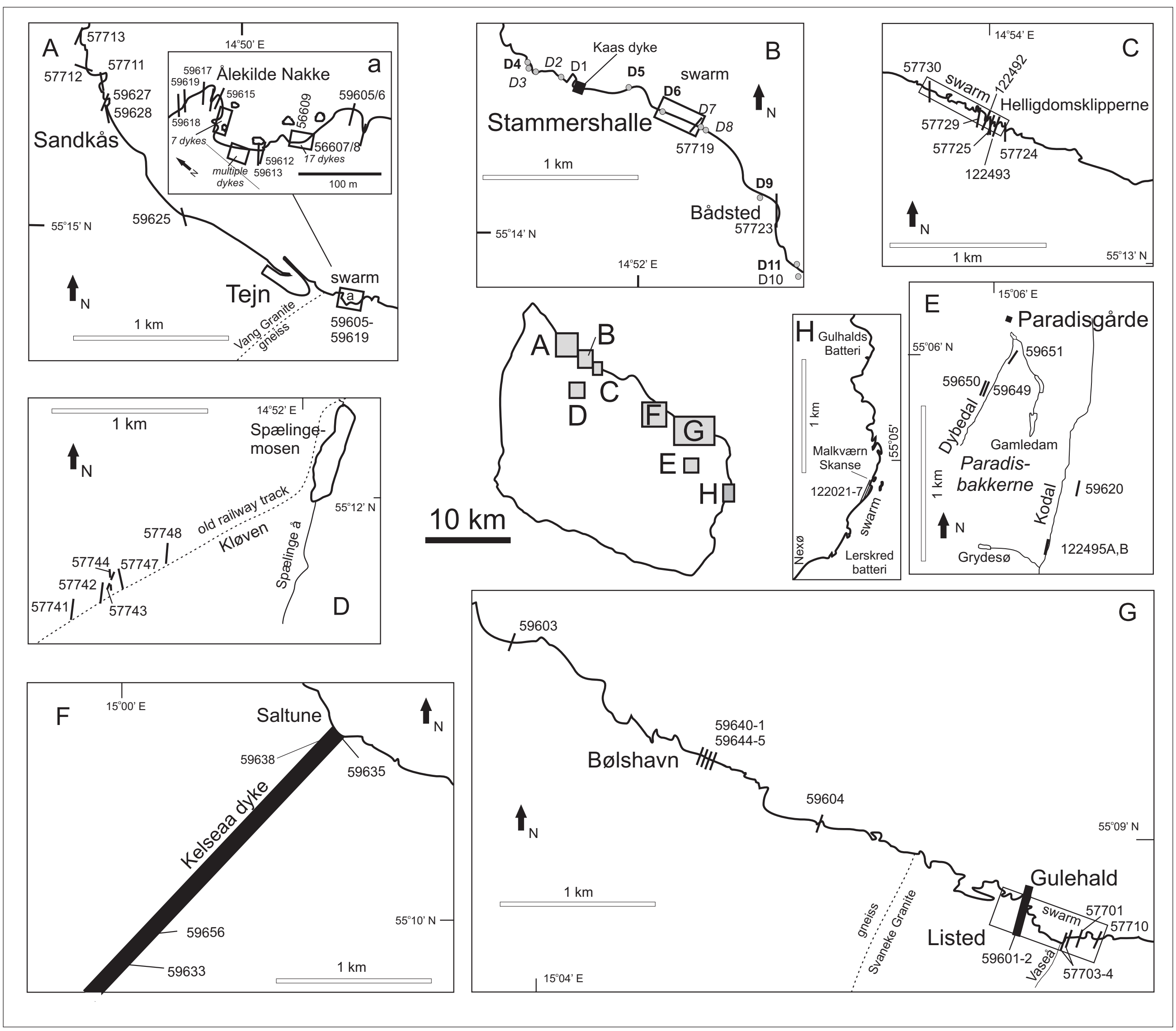

Figure 3: Location maps of the analyzed dyke samples. The positions of the detailed maps A-H are indicated in the central map of Bornholm. The inset (a) in (A) is an enlargement of the Tejn dyke swarm area. The locations of new samples and the dyke swarms as defined by Münther (1945a) are shown schematically. In B the approximate locations (marked D1, D2, etc.) of the samples used for palaeomagnetic age determination (Abrahamsen & Lewandowski, 1995) are shown. The Vang granite in (A) and Svaneke granite in (G) are two of the younger granites (see Fig. 1).

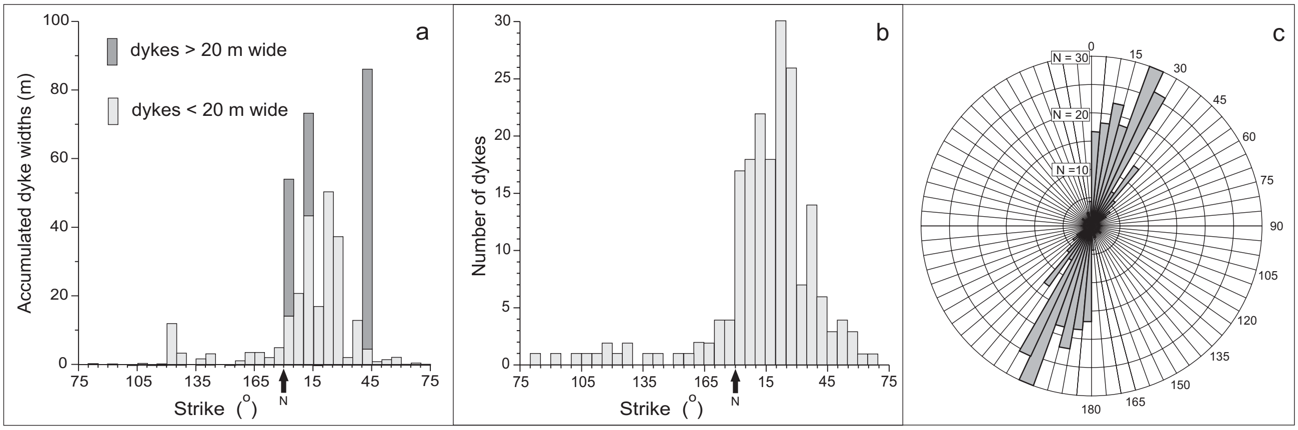

Figure 4: Distribution by orientation of the Bornholm dykes: (a) accumulated dyke widths per 5° strike intervals, (b) dyke frequency as a function of strike, and (c) Rose diagram of dyke frequency as a function of strike. NNE-striking dykes dominate in both number and width. Data from Münther (1945a).

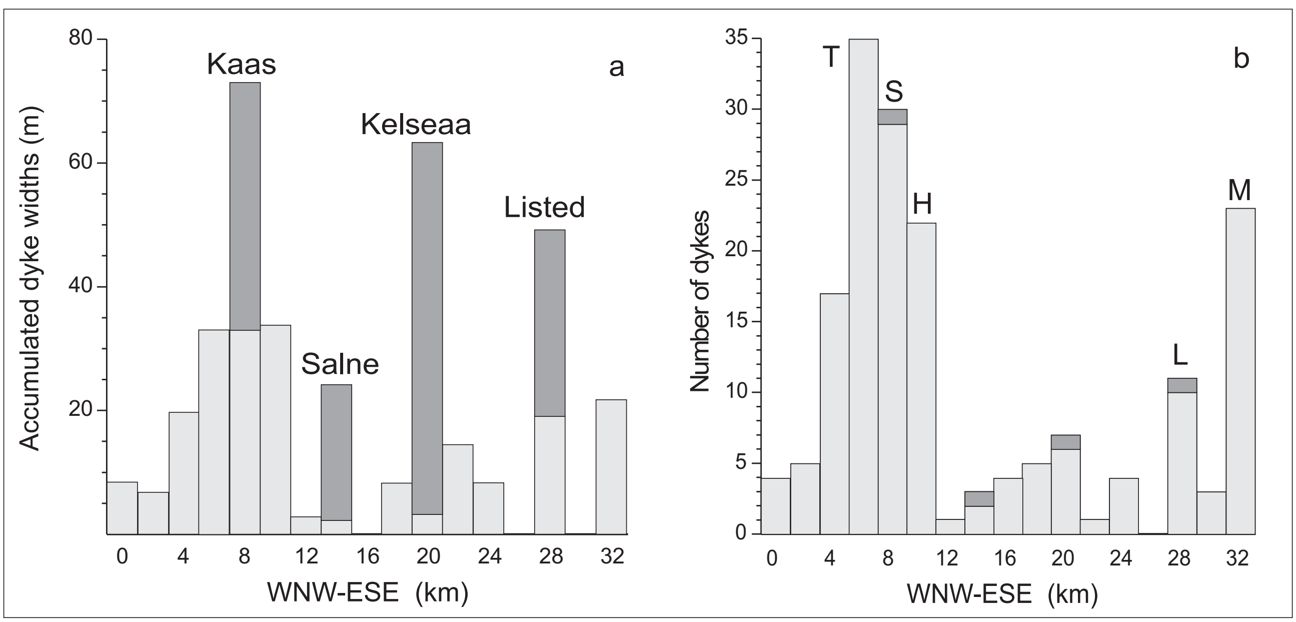

Figure 5: Distribution of the Bornholm dykes along a transect normal to the main orientation: (a) accumulated width per 2 km intervals and (b) frequency per 2 km intervals. Observations for the transect are mainly obtained along the north and east coasts of Bornholm with some contributions from inland locations and very few from the west coast. There is clearly an inhomogeneous distribution which led Münther (1945a) to define dyke swarms at (b): T – Tejn, S – Stammershalle, H – Helligdomsklipperne, L – Listed, and M – Malkværn Skanse. See text for discussion. The approximate locations of the four > 20 m wide dykes are shown with dark shading.

The four large dykes, Kelseaa, Kaas, Listed, and Salne, together make up a width of 152 m; the four dyke swarms have an accumulated width of 117 m; and 105 other individual dykes have a total width of 142 m wide according to the data of Münther (1945a, 1945b). This gives an absolute total dyke width of 411 m on Bornholm. We have analyzed 56 representative dykes with an aggregated width of 210 m out of the 411 m total. The dykes were sampled predominantly along the north coast of Bornholm but also at Kløven, Paradisbakkerne, along Kelse Å (Å = aa = stream) and along the east coast. Locations are shown in Fig. 3 and listed in Table 1.

On the basis of palaeomagnetic data Abrahamsen & Lewandowski (1995) concluded that Bornholm has remained in a fixed position relative to the Baltic Shield at least since the intrusion of the oldest dykes.

Table 1
Location and rock type of Bornholm dykes.

Sample	Area	Location	Width (m)	Strike	TAS field	Sub-field	CIPW norm ne, (q) (wt.%)
Kelseaa type (1)							
59633	Kelseaa	Kløvedal	60	40	basalt	medium-K ol tholeiite	0
59635	Kelseaa	Saltune	0.35	40	basalt	medium-K ol tholeiite	0
59656	Kelseaa	Hullegård	60	40	basalt	medium-K ol tholeiite	0
59638	Kelseaa	Saltune	-	-	basalt	ol tholeiite	0
57719	North coast	Stammershalle	1.7	42	basalt	ol tholeiite	0
Narrow dykes type (2)							
59644	North coast	Bølshavn	0.3	c. 20[1]	basalt	basaltic picrite	0
122022	East coast	Malkværn	3.1	25	basalt	basaltic picrite	0
59620	Paradisbakkkerne	Kodal	-	20	basalt	basaltic picrite	0
122025	East coast	Malkværn	0.7	25	basalt	alkali basalt	1
122023	East coast	Malkværn	0.35	25	basalt	alkali basalt	2
122021	East coast	Malkværn	0.6	25	basalt	alkali basalt	1
122026	East coast	Malkværn	0.4	25	basalt	ol tholeite	0
57751	Hammer granite	Sjælemose	0.4	12	basalt	medium-K ol tholeiite	0
122027	East coast	Malkværn	0.2	25	basalt	ol tholeite	0
122493	North coast	Helligdomsklipperne	0.5	10	basalt	medium-K ol tholeiite	0
122492	North coast	Helligdomsklipperne	2	20	basalt	medium-K ol tholeiite	0
57710	North coast	Vaseå	0.2	25	basalt	high-K ol tholeiite	0
57701	North coast	Vaseå	0.9	22	basalt	alkali basalt	5
59645	North coast	Bølshavn	2	c. 20[1]	basalt	alkali basalt	1
57748	Kløven	Old	0.7	4	basalt	alkali basalt	1
59618	North coast	Tejn	0.16	178	basalt	alkali basalt	3
59649	Paradisbakkkerne	Dybedal	0.35	24	basalt	alkali basalt	3
59612	North coast	Tejn	2.5	180	trachybasalt	hawaiite	2
59604	North coast	Helligkvinde	0.3	8	trachybasalt	hawaiite	6
59628	North coast	Storedal å	0.8	170	trachybasalt	hawaiite	2
59613	North coast	Tejn	0.3	22	trachybasalt	hawaiite	2
57724	North coast	Helligdomsklipperne	2	10	trachybasalt	hawaiite	0
59627	North coast	Sandkås	2	25	trachybasalt	potassic trachybasalt	1
59640	North coast	Bølshavn	0.7	c. 20[1]	trachybasalt	potassic trachybasalt	6
57711	North coast	Sandkås	0.65	170	trachybasalt	potassic trachybasalt	0
59650	Paradisbakkkerne	Dybedal	0.3	24	trachybasalt	potassic trachybasalt	5
59651	Paradisbakkkerne	Paradisgårde	0.4	34	trachybasalt	potassic trachybasalt	3
59619	North coast	Tejn	0.1	178	trachybasalt	potassic trachybasalt	2
59605	North coast	Tejn	0.4	14	trachybasalt	potassic trachybasalt	1
59606	North coast	Tejn	0.4	14	trachybasalt	potassic trachybasalt	0
59609	North coast	Tejn	2.5	22	trachybasalt	potassic trachybasalt	0
122495A	Paradisbakkkerne	Kodal	0.2	12	tephrite/basanite	basanite	1
57725	North coast	Helligdomsklipperne	2	20	tephrite/basanite	basanite	8
57729	North coast	Helligdomsklipperne	2	13	tephrite/basanite	basanite	6
59625	North coast	Sandkås	2.5	164	tephrite/basanite	basanite	4
122495B	Paradisbakkkerne	Kodal	0.1	12	tephrite/basanite	basanite	1
57741	Kløven		1.3	6	tephrite/basanite	basanite	4
57730	North coast	Helligdomsklipperne	1.2	13	phonotephrite	phonotephrite	5
57743	Kløven		0.65	178	phonotephrite	phonotephrite	3
57747	Kløven		0.5-3	169	phonotephrite	phonotephrite	4
Enriched narrow dykes type (2*)							
57703	North coast	Vaseå	0.7	22	basanite	potassic basanitic picrite	5
57704	North coast	Vaseå	0.3	22	basanite	potassic basanitic picrite	5
59607	North coast	Tejn	2	22	trachybasalt	potassic trachybasalt	6
59608	North coast	Tejn	2	22	trachybasalt	potassic trachybasalt	4
59615	North coast	Tejn	1	23	trachybasalt	potassic trachybasalt	5
59617	North coast	Tejn	0.1	24	trachybasalt	potassic trachybasalt	5
Kaas dyke type (3)							
57714	North coast	Kaas dyke	40	158	basaltic trachyandesite	shoshonite	(6)
57715	North coast	Kaas dyke	40	160	basaltic trachyandesite	mugearite	(1)
57750	North coast	Kaas	32	c. 160[1]	trachbasalt	potassic trachybasalt	(2)
57713	North coast	Sandkås	-	24	trachbasalt	potassic trachybasalt	(2)
57742	Kløven		0.8	20	basaltic trachyandesite	shoshonite	(3)
57744	Kløven		0.8	178	basaltic trachyandesite	shoshonite	(7)
Listed dyke (3)							
59601	North coast	Gulehald, Listed	30	14	basaltic trachyandesite	mugearite	(5)
59602	North coast	Gulehald, Listed	30	14	basaltic trachyandesite	mugearite	(4)
NW trending dyke (4)							
57712	North coast	Sandkås	1	110	basalt	medium-K quartz tholeiite	(5)

Footnote:
-) unknown due to insufficient outcrop
1) estimated strike due to insufficient outcrop

Age relations of the dykes and their relations to southern Sweden

Traditionally, the dykes have been considered to be related to major Proterozoic dyke swarms in southern Sweden (Berthelsen, 1989), e.g. the Central Scandinavian Dolerite Group (CSDG) and the Blekinge Dalarne Dolerite Group (BDDG) (e.g. Gorbatschev et al., 1979; Solyom et. al., 1992; Patchett et al., 1994).

Although the geochronology of the Bornholm dykes is poorly constrained, geological relations and palaeomagnetic and isotopic dating allow some inferences to be made. Some of the dykes, both large (Kelseaa and Listed) and small, cut the younger granites (Fig. 1), whereas the dykes in Paradisbakkerne cut the Paradisbakkerne migmatite. Most of the dykes are intruded into grey gneisses. The Listed dyke is cut by what has been referred to as 'sandstone dykes', which are sand-filled fractures in the basement rocks. The sandstone in these fractures is related to the Early Cambrian Nexø sandstone, the earliest preserved sedimentary deposit on Bornholm (Bruun-Petersen, 1975; Lewandowsky & Abrahamsen, 2003).

An U-Pb age of 1326 ±10 Ma (2σ) was obtained on baddeleyite from the Kelseaa dyke (Holm et al., 2005) in accordance with a previously published, less precise, estimate based on palaeomagnetic data (Abrahamsen, 1977). Further palaeomagnetic investigations of a suite of dykes from primarily two areas on Bornholm (Stammershalle and Listed), revealed that narrow NNW- to NNE-trending dykes were intruded around 1220 Ma, whereas the Kaas and Listed dykes were emplaced at c. 950 Ma with a possibility that the Listed dyke cooled at c. 700 - 800 Ma (Abrahamsen, 1977; Abrahamsen & Lewandowski, 1995). This links most of the dyke intrusions with two important igneous units in Sweden, the Protogine Zone Dolerite Group (PZDG, 1215-1221 Ma) and the Blekinge Dalarne Dolerite Group (BDDG, 100-870 Ma), respectively. A few dykes that trend WNW to NW seem to be of Permian age (Abrahamsen & Lewandowski, 1995). These have been described by Jensen (1988) and Obst (2000), who also consider them to be related to Permian dykes in Scania, southern Sweden (Fig. 1). Bornholm is situated along strike from the Scania dykes and their correlation seems straightforward.

Palaeomagentic and U-Pb results from Bornholm (Abrahamsen, 1977; Abrahamsen & Lewandowski, 1995; Holm et al. 2005) suggest at least four episodes of dyke injection: 1326 Ma (Kelseaa), c. 1220 Ma (some narrow dykes), c. 950 Ma (Kaas, and possibly Listed), and around 300 Ma (WNW- to NW-trending dykes). The fault pattern on Bornholm further suggests at least four episodes of horizontal movement (Münther, 1945a, 1945b) during which dyke emplacement could have occurred. As shown below, the geochemistry of the dykes may likewise be assigned to a number of discrete episodes of mafic magmatism, each with their own distinct character.

Three episodes of dyke emplacement have been recognized in southern Sweden (Fig. 1). The PZDG occurs in a 20 km-wide tectonic belt that extends N and NNE from southern Sweden into the central part of Scania (Klingspor, 1976). The age range of these dykes has been recently demonstrated by U-Pb analysis of baddeleyite to be 1215-1221 Ma (Söderlund et al., 2005). The BDDG extends over an area 700 km long and 150 km wide east of and parallel to the Protogine Zone and trend NNE north of Bornholm (Fig. 1). The intrusion age interval is indicated to be 1000 – 870 Ma (Patchett, 1978), and perhaps close to 930 Ma (Johansson & Johansson, 1990). The Permo-Carboniferous WNW- to NW-trending Scania dykes are widely distributed in the basement of central Scania (Klingspor, 1976). Dykes from a fourth mafic intrusive event that took place at 1270-1250 Ma are present in mid Sweden and western Finland, around 600 km to the north of Bornholm; this is the Central Scandinavian Dolerite Group (CSDG) (Söderlund et al., 2006).

Petrography

The petrographic descriptions below are based on our study of new samples combined with the detailed descriptions of some of the dykes mentioned by Callisen (1934) and Jensen (1966).

Petrographically we can divide the dykes into four main types: 1) Kelseaa type, 2) narrow dykes, 3) large dykes at Kaas and Listed, and 4) WNW- to NW-trending dykes (in the following referred to simply as the NW dykes). The relatively unaltered state of the Bornholm dykes in general is demonstrated by the common occurrence of well-preserved primary igneous minerals such as olivine and clinopyroxene.

Kelseaa

The Kelseaa dyke is a remarkably fresh, grey, massive rock (Fig. 6). The grain size varies from fine to medium and the texture is ophitic near the contact and coarsely gabbroic in the centre. Plagioclase, olivine (Fo_{60}), and augite are the main constituents with accessory amounts of Ti-magnetite, apatite, hypersthene, green uralitic amphibole, biotite, microcline, and quartz. Plagioclase in the centre of the dyke is zoned from labradorite (An_{70}) to oligoclase (An_{20}). Bytownite (An_{83}) and hypersthene occur near the contact. In the centre

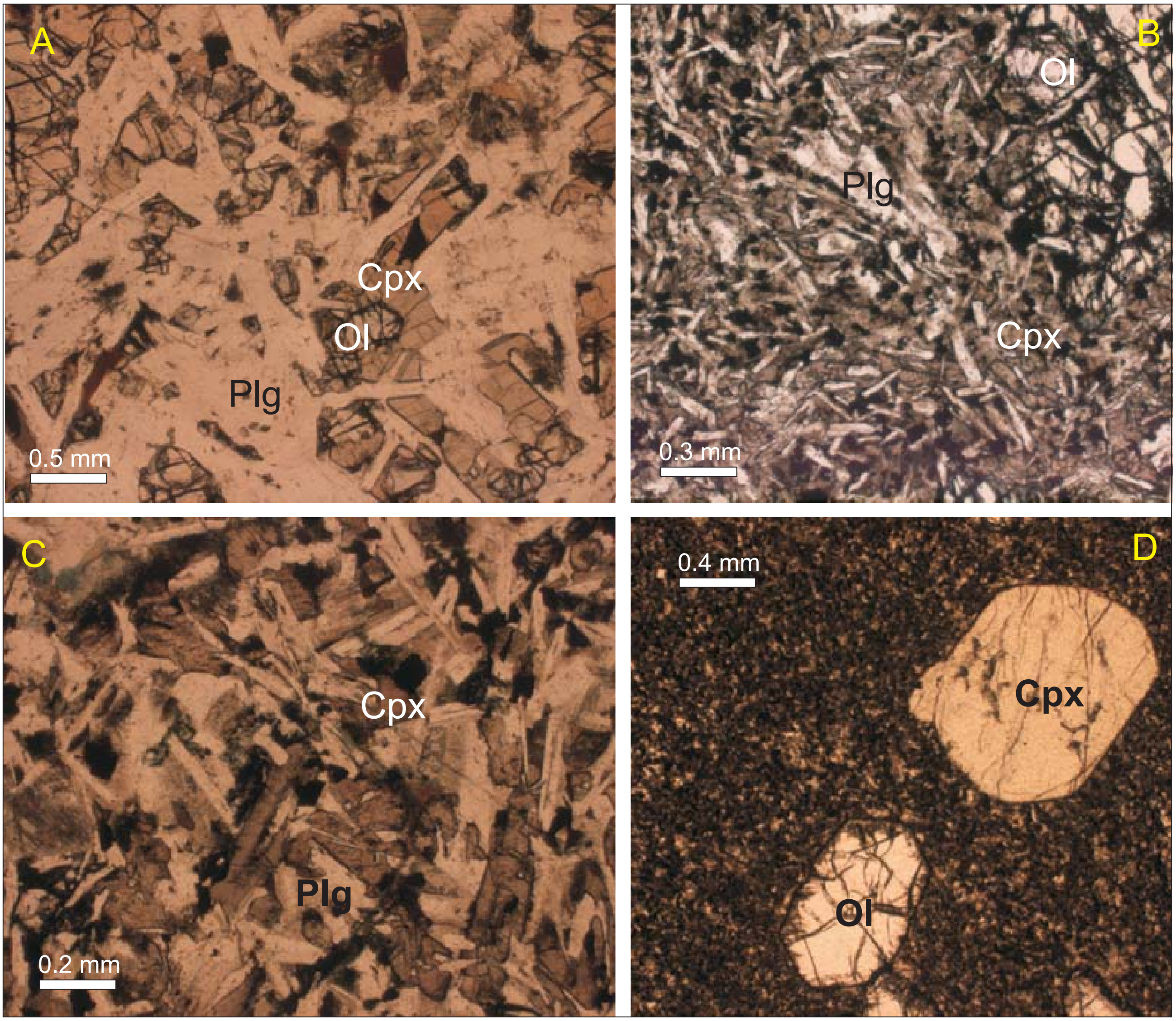

Figure 6: Photomicrographs (plane polarized light) of mafic dykes from Bornholm. A) the tholeiitic Kelseaa dyke (type 1) sample 59635: B-D alkaline dykes: B) narrow dyke 57751 (Type 2), C) narrow dyke 59605 (Type 2), D) enriched narrow dyke 59617 (Type 2*). Examples of minerals are indicated: ol – olivine, cpx – clinopyroxene, plg – plagioclase. See Tables 1 & 2 and text for details. Groups 3 and 4 are illustrated by Callisen (1934) and Jensen (1966).

small patches of fine grained microcline, oxides, and quartz occur interstitally between plagioclase laths, and are probably fractionation products. Small amounts of serpentine, chlorite, epidote and calcite are present as alteration products.

The narrow dykes

The narrow dykes are all fine grained; some are porphyritic and some are aphyric. The porphyritic samples all have less than 5 vol% phenocrysts. Two different phenocryst assemblages are present: (1) olivine (or pseudomorphs after olivine) and/or clinopyroxene (Fig. 6), or (2) olivine (or pseudomorphs) and plagioclase. The groundmass in the narrow dykes consists mainly of plagioclase, clinopyroxene and Fe-Ti oxide.

The Kaas-Listed dykes

The petrography of these evolved large dykes (Jensen, 1966) is quite similar to the Kelseaa dyke, but they do not have the coarse grained gabbroic central part. They have ophitic textures and are composed mainly of plagioclase, augite and olivine. The plagioclase is zoned from labradorite to oligoclase. Minor constituents are Fe-Ti oxides, biotite, quartz, and brown hornblende. Graphic intergrowths of quartz and feldspar in the rims of plagioclase laths are common in the centre of the Kaas dyke. Augite is absent near the contact of this dyke, whereas in the Listed dyke olivine is absent near the contact.

The Listed dyke has a 3-4 m wide zone near the contact containing numerous elliptical plagioclase crystals or crystal aggregates. The presence of these plagioclase ovoids has been interpreted as resulting from the assimilation of country rock (Callisen, 1934; Jensen, 1966). However, as the large feldspar crystals in the wall rock are alkali feldspar, the plagioclase ovoids, if xenocrystic, must originate from a different rock type located deeper in the crust (Berthelsen, 1989). The zone of ovoids terminates abruptly towards the center of the dyke, implying that multiple intrusion has occurred.

NW-trending dykes

These relatively few basaltic dykes are plagioclase and clinopyroxene phyric, sometimes including small amounts of olivine. Phenocrysts often show resorption. Obst (2000) has described a 12 m-wide dolerite dyke that can be traced for over 3 km from Lindesdal. A trachytic dyke with the same trend is included in this group (Obst, 2000), and this dyke was suggested to be closely related to the so-called kullaites in NW Scania (Jensen, 1988).

Analytical methods

Sixty samples have been analyzed for major and trace elements by XRF. Major element analyses were acquired at the Geological Survey of Denmark and Greenland (GEUS) in Copenhagen. Analyses were made on glass discs prepared with sodium borate, except for Na_2O and MgO (atomic absorption), FeO (titration) and volatiles (calculated from loss on ignition).

Trace elements were determined by XRF (Rb, Ba, Sr, La, Ce, Nd, Y, Th, Zr, Nb, Zn, Cu, Co, Ni, Sc, V, Cr, and Ga) and 26 samples were additionally analyzed by INAA (La, Ce, Nd, Sm, Eu, Tb, Yb, Lu, U, Th, Ta, and Hf) by R. Gwozdz (Tracechem, Copenhagen), and 7 samples by ICP-MS (Sc, V, Cr, Co, Ni, Cu, Zn, Ga, Rb, Sr, Y, Zr, Nb, REEs, Hf, Ta, and Th) at Actlabs ©. The data is presented in Table 2. The major elements have been recalculated to 100 % on a volatile free basis. Analytical details are given in the appendix.

Geochemistry

Introduction

The mafic dykes on Bornholm are classified according to the IUGS classification using total alkali-silica (TAS) (Le Maitre et al., 1989; Le Bas, 2000). The rock classification (Fig. 7) is further detailed in Table 1. The majority of them range from basalts through alkali basalts (nepheline normative, Table 1) and trachybasalts to basanites. Potassic types dominate and most are nepheline CIPW normative, but sodic rocks (hawaiites) do occur, and three picrites are reported (Table 1). The compositions extend to very evolved types with a total range of MgO = 14.2 - 2.1 wt. % (Fig. 8). All major element analyses are in wt. % and will be expressed below as %. A total of 42 of the analyzed dykes are rather primitive with MgO > 5.8 %, and of these 30 have Mg# = 60 – 74 (Mg# = $Mg/(Mg+Fe^{2+})$ (atoms/atoms), Mg# calculated assuming FeO/FeO^{total} = 0.8 (Middlemost, 1989)), > 130 ppm Ni and > 225 ppm Cr (Figs. 8 & 9, Table 2). Silica concentrations for these rocks are 44 - 50 %. Fifteen of the dykes are more evolved with MgO = 2.1 – 5.5 %, and silica reaching 57 %. The relatively primitive nature of most of the dykes is in marked contrast to the distribution of compositions of the Swedish Proterozoic dykes which are generally quite evolved with just a small fraction exceeding 8 % MgO (Solyom et al., 1992).

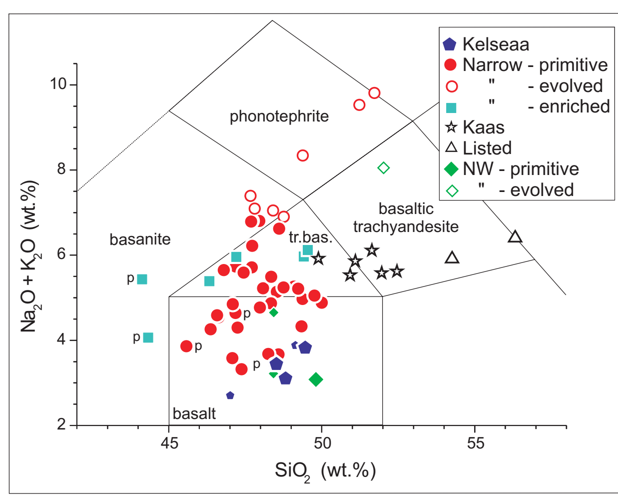

Figure 7: $Na_2O + K_2O$ vs. SiO_2 (TAS diagram) for the Bornholm dykes with the IUGS classification according to Le Maitre (1989) and Le Bas (2000); tr. bas. – trachybasalt. Filled symbols: rocks with MgO > 5.8 %, open symbols: evolved rocks (MgO < 5.8 %), small diamonds (3): NW-trending dykes from Jensen (1988) and Obst (2000); small hexagons (2): Kelseaa dolerite-like dykes; picrite samples are denoted by "p"; NW in legend: NW- to WNW-trending dykes. Rocks are further characterized in Table 1, and analytical data listed in Table 2.

Table 2
Geochemical compostion of Bornholm dykes

Sample id	59633	59635	59656	59638	57719	59644	122022	59620	122025	122023	122021	122026	57751	122027	122493	122492	57710
Location	Kelseaa	Kelseaa	Kelseaa	Cuts Kelseaa	Stammershl	Bølshavn	Malkværn	Paradisbk	Malkværn	Malkværn	Malkværn	Malkværn	Sjælemose	Malkværn	Helligdom	Helligdom	Vaseå
Type	1	1	1	1	1	2	2	2	2	2	2	2	2	2	2	2	2
Major elements (wt.%)																	
SiO_2	49.46	48.82	48.52	47.27	47.01	47.18	45.58	48.46	46.37	46.58	46.63	47.08	49.14	47.38	48.25	48.59	49.34
TiO_2	0.91	0.46	0.88	1.28	1.00	1.67	1.28	1.31	1.72	1.72	2.00	1.84	1.23	1.64	1.42	1.38	1.51
Al_2O_3	15.83	18.93	15.66	12.22	16.47	13.20	13.51	12.52	14.00	14.60	14.65	13.57	15.19	14.12	13.34	13.42	13.02
FeO^{total}	10.87	8.56	11.63	15.45	12.71	11.79	10.99	12.29	10.77	11.41	11.36	11.64	10.90	12.06	11.61	11.75	11.27
MnO	0.18	0.13	0.18	0.24	0.24	0.20	0.16	0.22	0.17	0.23	0.30	0.25	0.16	0.33	0.21	0.30	0.23
MgO	8.60	9.21	9.94	12.00	7.94	12.64	14.24	12.74	11.61	11.00	9.71	11.33	9.83	10.55	11.38	10.66	10.75
CaO	9.81	10.51	9.24	7.40	11.44	7.66	7.86	8.51	8.18	7.86	7.67	8.13	9.15	7.51	8.67	8.77	9.13
Na_2O	2.65	2.32	2.37	2.15	2.25	2.37	2.16	2.42	2.63	2.85	2.94	2.31	3.00	2.36	2.64	2.60	2.66
K_2O	1.17	0.78	1.06	1.25	0.45	2.26	1.70	1.01	1.63	1.75	1.60	1.27	0.88	0.95	1.04	1.07	1.66
P_2O_5	0.18	0.07	0.14	0.18	0.10	0.29	0.28	0.18	0.31	0.34	0.30	0.20	0.19	0.16	0.16	0.16	0.20
sum	100.00	100.00	100.00	100.00	100.00	100.00	98.98	100.00	98.58	99.60	98.44	98.90	100.00	98.41	100.00	100.00	100.00
volatiles	2.52	1.24	2.38	3.38	5.43	4.18	4.12	3.99	3.50	3.79	3.97	3.40	3.06	3.43	2.34	2.89	3.21
Fe^{2+}/Fe^{total}	0.72	0.78	0.72	0.68	0.72	0.44		0.75					0.73				0.82
Mg# (Fe^{2+}/Fe^{total} = 0.8)	64	71	66	63	58	70	74	70	71	68	66	68	67	66	69	67	68
Trace elements (ppm)																	
Sc	27	16	*28*	28	*24*	19	*22*	18	*23*	*22*	*23*	*23*	21	*22*	21	20	25
V	214	126	*179*	324	*246*	189	*152*	174	*194*	*195*	*205*	*211*	179	*217*	202	199	202
Cr	390	409	*314*	228	*364*	451	*699*	526	*674*	*520*	*531*	*632*	474	*570*	466	471	859
Co	67	76	*70*	90	*77*	74	*72*	86	*73*	*65*	*64*	*71*	65	*68*	65	67	73
Ni	259	310	*243*	430	*313*	393	*386*	480	*342*	*270*	*261*	*342*	257	*342*	357	384	267
Cu	114	109	*114*	117	*177*	177	*52*	76	*62*	*42*	*52*	*62*	59	*62*	66	63	59
Zn	84	59	*55*	101	*126*	134	*104*	117	*207*	*125*	*115*	*197*	78	*124*	108	109	125
Ga	20	15	*17*	19	*19*	20	*17*	16	*22*	*20*	*21*	*19*	19	*20*	19	19	19
Rb	50	33	*48*	60	*27*	172	47	64	58	52	51	42	37	34	69	73	124
Sr	145	148	*119*	111	*143*	142	561	385	595	635	604	423	464	359	397	389	426
Y	38.9	18.2	*32.2*	40	*29*	17	*9.39*	17.8	*15.55*	*11.44*	*16.67*	*14.5*	18.6	*12.43*	16.2	15.9	26.9
Zr	126	66	*103*	130	*91*	44	*117*	81	*138*	*148*	*134*	*96*	91	*106*	81	79	105
Nb	6.6	3.5	*4.0*	6.3	*0.6*	26.0	*15.7*	13.6	*18.7*	*18.7*	*19.8*	*14.5*	10.4	*10.4*	12.8	13.1	17.6
Ba	351	225	*370*	338	*71*	651	629	286	510	556	580	349	262	351	322	368	348
La	13.3	9.1	*10.10*	14.5	*1.47*	22.9	*21.1*	11.5	*25.3*	*25.5*	*26.0*	*13.3*	11.4	*10.7*	11.8	10.9	20.7
Ce	30.7	14.1	*20.80*	29.9	*3.47*	45.8	*43.9*	19.9	*52.8*	*53.8*	*54.6*	*29.5*	31.1	*24.3*	28.8	28.9	41.3
Nd	16.4	8.1	*11.40*	16.5	*3.81*	29.2	*19.0*	13.6	*22.7*	*23.1*	*23.8*	*15.5*	18.6	*14.3*	16.2	16.4	22.7
Sm	3.79	1.97	*3.09*		*1.87*		*3.86*	3.18	*4.87*	*4.78*	*5.21*	*3.83*	3.37	*3.63*			4.11
Eu	1.26	0.67	*1.04*		*0.83*		*1.31*	1.08	*1.60*	*1.58*	*1.77*	*1.35*	1.23	*1.24*			1.40
Tb	1.06	0.43	*0.75*		*0.48*		*0.52*	0.53	*0.62*	*0.62*	*0.73*	*0.62*	0.58	*0.52*			0.79
Yb	2.64	1.60	*2.53*		*1.19*		*0.94*	1.39	*1.35*	*1.25*	*1.35*	*1.35*	1.53	*1.45*			1.75
Lu	0.30	0.19	*0.37*		*0.18*		*0.17*	0.17	*0.19*	*0.17*	*0.20*	*0.19*	0.19	*0.20*			0.22
Hf	3.12	1.58	*2.39*		*1.31*		*3.23*	2.10	*3.84*	*4.05*	*3.75*	*2.80*	2.12	*3.42*			2.57
Ta	0.38	0.29	*0.39*		*0.06*		*1.04*	0.71	*1.24*	*1.35*	*1.35*	*0.93*	0.59	*0.73*			1.01
Th	2.7	2.0	*2.0*	2	*0.04*	1	*1.3*	1.0	*1.5*	*1.6*	*1.6*	*0.9*	1.2	*0.8*	1	1	2.4

Analytical method for trace elements: Normal font - XRF, italics - ICPMS, underlined - INAA. 1) T.E. Waight (pers. comm.) BH3A: North Coast, 50 m E of Kelseaa dyke, BH22: Dalegård Quarry, Olsker.

Table 2. Continued

Sample id Location Type	57701 Vaseå 2	59645 Bølshavn 2	57748 Kløven 2	59618 Tejn 2	59649 Paradisbk 2	59612 Tejn 2	59604 Helligkvinde 2	59628 Sandkås 2	59613 Tejn 2	57724 Helligdom 2	59627 Sandkås 2	59640 Bølshavn 2	57711 Sandkås 2	59650 Paradisbk 2	59651 Paradisbk 2	59619 Tejn 2	59605 Tejn 2	59606 Tejn 2
SiO_2	47.09	47.25	47.98	48.34	49.23	46.80	47.45	47.71	48.53	48.76	47.19	47.73	48.08	48.35	48.75	49.09	49.37	49.76
TiO_2	1.95	1.72	1.90	1.62	1.87	1.93	2.19	2.55	1.83	2.82	2.18	2.08	2.33	2.04	2.15	1.68	1.91	1.95
Al_2O_3	13.37	13.43	16.72	13.55	14.80	16.25	16.44	16.27	15.91	18.90	15.56	15.97	16.78	13.87	14.43	14.27	15.10	15.38
FeO^{total}	11.72	12.03	11.84	11.18	11.12	15.01	15.17	12.64	11.50	13.92	14.89	12.05	12.50	11.75	11.54	11.23	11.01	11.13
MnO	0.17	0.19	0.26	0.26	0.15	0.18	0.35	0.19	0.15	0.19	0.47	0.30	0.18	0.16	0.16	0.47	0.16	0.17
MgO	10.42	11.87	7.77	10.38	7.84	6.12	5.64	6.10	8.76	5.06	8.17	7.14	8.32	8.87	8.12	9.08	7.80	6.81
CaO	9.79	8.50	8.24	9.23	9.20	7.19	7.03	8.06	7.60	2.80	5.53	7.83	6.03	8.92	9.00	8.32	9.04	9.09
Na_2O	2.78	2.56	3.16	3.08	3.58	3.74	3.80	3.57	3.72	4.94	3.66	3.68	3.37	3.43	3.48	3.30	3.37	3.42
K_2O	2.07	1.73	1.61	1.79	1.62	1.91	1.79	2.15	1.42	1.95	2.07	2.54	1.86	2.06	1.76	1.96	1.60	1.63
P_2O_5	0.28	0.31	0.25	0.26	0.26	0.33	0.31	0.38	0.30	0.42	0.35	0.35	0.33	0.30	0.30	0.29	0.34	0.35
sum	100.00	100.00	99.99	100.00	100.00	100.00	100.00	100.00	100.00	100.00	100.00	100.00	100.00	100.00	100.00	100.00	100.00	100.00
volatiles	3.33	5.54	6.93	3.17	2.32	6.46	4.94	8.07	2.93	4.83	5.17	6.78	6.44	3.17	3.01	3.32	2.86	3.15
Fe^{2+}/Fe^{total}	0.72	0.70	0.80	0.75	0.74	0.66		0.72	0.80	0.84		0.75	0.84	0.81	0.74	0.75	0.75	0.75
Mg#	66	69	59	67	61	48	45	52	63	45	55	57	60	63	61	64	61	58
Sc	19	18	25	19	15	29	23	21	13	18	18	21	20	15	16	20	20	19
V	195	200	183	190	193	245	293	213	124	119	153	239	175	190	201	202	177	184
Cr	455	477	277	504	319	529	113	353	292	13	234	370	364	394	358	480	302	307
Co	66	72	61	70	56	68	62	58	71	55	76	54	68	69	60	70	61	63
Ni	270	361	161	309	150	220	59	234	186	44	178	145	185	228	185	269	184	186
Cu	71	10	42	66	57	60	45	51	35	21	31	58	37	59	58	61	51	58
Zn	82	148	103	111	105	140	129	129	78	218	133	172	152	106	110	137	89	101
Ga	20	21	18	22	22	24	24	25	22	24	24	25	22	25	24	21	21	24
Rb	63	100	95	52	53	57	55	83	31	59	67	151	85	77	86	61	34	35
Sr	619	533	569	599	604	645	553	596	732	603	731	561	666	645	662	603	569	575
Y	20.7	20.2	21.6	20.7	21.5	31.2	25.4	28	16.5	35.8	17.9	33.4	23.7	21.8	20.6	23.9	23.8	25.9
Zr	116	115	122	116	124	129	123	174	143	201	176	151	168	133	133	124	155	162
Nb	24.8	25.5	14.0	22.8	22.5	26.9	28.5	26.0	19.6	31.6	23.2	33.4	20.4	24.9	25.8	23.9	24.8	24.9
Ba	524	560	394	522	476	577	595	548	500	606	647	801	434	508	514	568	511	524
La	20.7	24.5	15.1	21.8	20.5	23.7	25.4	27.0	19.6	25.2	28.4	31.3	22.6	21.8	22.7	23.9	22.7	23.8
Ce	40.3	47.9	34.5	46.7	42.0	52.8	47.5	52.0	43.3	57.9	58.9	62.6	45.2	44.6	47.5	46.7	44.4	50.8
Nd	24.8	27.7	22.6	27.0	23.6	28.0	27.5	35.0	26.8	32.6	33.7	34.5	26.9	25.9	26.8	28.0	25.8	28.0
Sm	4.79	4.49		4.58		4.97	4.83		4.40		5.53		5.03	4.99	5.22			5.30
Eu	1.67	1.60		1.52		1.60	1.69		1.53		1.85		1.94	1.63	1.66			1.71
Tb	0.61	0.65		0.62		0.79	0.69		0.70		0.71		0.84	0.72	0.75			0.80
Yb	1.30	1.00		1.49		2.33	1.53		1.24		1.32		1.48	1.59	1.45			1.93
Lu	0.17	0.14		0.20		0.25	0.18		0.15		0.16		0.20	0.18	0.19			0.27
Hf	2.86	2.63		2.90		3.12	2.76		3.48		4.23		3.68	3.40	3.39			4.04
Ta	1.45	1.58		1.16		1.43	1.59		1.09		1.18		1.11	1.38	1.44			1.28
Th	2.5	1.9	1	2.1	3	2.0	1.9	3	1.1	1	1.4	1	1.3	2.1	2.2	1	1	2.0

Table 2. Continued

Sample id Location Type	59609 Tejn 2	122495A Paradisbk 2	57725 Helligdom 2	57729 Helligdom 2	59625 Sandkås 2	122495B Paradisbk 2	57741 Kløven 2	57730 Helligdom 2	57743 Kløven 2	57747 Kløven 2	57703 Vaseå 2*	57704 Vaseå 2*	59607 Tejn 2*	59608 Tejn 2*	59615 Tejn 2*	59617 Tejn 2*	57714 Kaas dyke 3	57715 Kaas dyke 3
SiO_2	50.00	47.67	47.69	47.81	47.96	48.41	48.61	49.38	51.23	51.72	44.33	44.13	46.33	47.21	49.41	49.55	51.64	51.10
TiO_2	1.76	2.70	2.41	2.53	2.30	2.71	2.39	2.92	1.65	1.60	2.50	2.40	2.44	2.56	1.99	2.04	3.96	3.04
Al_2O_3	14.25	18.23	16.35	17.09	16.38	18.19	16.58	17.67	18.07	18.40	12.37	12.18	13.10	14.57	12.34	12.64	16.35	15.72
FeO^{total}	11.41	13.08	11.78	12.43	12.01	12.84	12.15	12.79	11.72	11.43	12.87	12.70	12.96	13.07	10.67	10.62	12.03	11.80
MnO	0.14	0.19	0.16	0.17	0.15	0.23	0.22	0.19	0.18	0.27	0.18	0.21	0.17	0.15	0.17	0.17	0.08	0.14
MgO	8.11	4.76	6.99	4.73	7.05	4.54	6.11	3.88	2.24	2.09	13.36	13.92	9.57	7.09	10.22	9.41	2.93	5.40
CaO	8.73	4.11	7.11	6.70	6.49	4.16	6.37	3.93	3.67	2.98	9.72	8.46	9.15	8.45	8.56	8.74	5.45	5.95
Na_2O	3.45	4.09	4.25	4.83	3.99	4.72	4.40	4.85	4.88	5.58	1.68	1.12	3.20	3.58	3.41	3.42	3.79	3.97
K_2O	1.43	3.30	2.54	2.25	2.81	2.33	2.22	3.49	4.65	4.23	2.38	4.31	2.19	2.38	2.55	2.70	2.32	1.89
P_2O_5	0.25	0.42	0.46	1.15	0.59	0.43	0.59	0.55	1.18	1.22	0.30	0.30	0.42	0.46	0.43	0.44	0.96	0.67
sum	100.00	100.00	100.00	100.00	100.00	100.00	100.00	100.00	100.00	100.00	100.00	100.00	100.00	100.00	100.00	100.00	100.00	100.00
volatiles	3.52	2.19	5.26	4.03	4.42	2.89	4.15	2.45	2.59	2.13	4.86	4.19	3.51	3.15	2.78	2.47	1.98	2.51
Fe^{2+}/Fe^{total}	0.63		0.80	0.78	0.80		0.74	0.76	0.59	0.63	0.78	0.80	0.67	0.67	0.80	0.78	0.62	0.76
Mg#	61	45	57	46	57	44	53	40	30	29	70	71	62	55	68	66	35	50
Sc	16	16	18	16	18	17	14	9	8	7	19	18	16	16	16	17	27	16
V	208	127	138	89	141	108	121	65	8	7	256	243	192	219	162	174	209	167
Cr	444	9	225	90	239	7	167	7	4	1	481	525	339	328	410	395	39	155
Co	73	54	53	44	51	51	54	49	30	29	78	81	71	66	63	60	54	69
Ni	336	38	130	67	147	36	114	23	8	6	389	417	255	204	296	269	41	88
Cu	64	32	36	42	50	29	40	28	27	20	61	66	63	63	51	67	17	30
Zn	112	155	80	125	103	142	145	99	138	136	111	119	102	163	114	115	180	121
Ga	23	23	22	23	23	23	22	22	29	28	20	21	24	27	20	21	26	23
Rb	36	81	78	50	78	64	88	120	131	110	228	429	65	58	63	64	39	56
Sr	590	599	814	887	727	701	864	914	531	493	519	384	907	915	753	791	564	600
Y	17	32.8	21.2	27.1	20	24.2	18.9	30.9	36.1	34.9	20	20.9	21.9	20	25.8	25.8	44.9	32.8
Zr	106	185	209	200	186	190	214	240	394	401	122	122	149	146	182	183	332	241
Nb	21.0	29.1	29.6	34.5	29.0	29.9	32.6	36.0	58.8	60.5	32.6	32.3	39.6	42.0	40.2	41.3	20.4	19.5
Ba	443	582	637	731	710	747	909	830	1609	1406	700	655	868	1020	765	813	761	673
La	18.0	26.3	29.6	39.7	32.0	27.6	33.6	39.1	61.9	61.6	20.0	22.9	29.1	31.0	37.1	35.1	35.7	28.7
Ce	42.0	62.9	68.8	87.7	67.0	62.8	75.6	82.3	138.2	130.3	43.1	45.9	60.4	64.0	65.0	66.1	86.7	67.7
Nd	22.0	34.1	36.0	49.1	35.0	34.7	39.9	46.3	72.2	70.8	26.3	25.0	33.3	36.0	35.1	37.2	56.1	40.0
Sm								7.09	11.80	10.70	4.82		6.19		6.56		9.90	7.53
Eu								2.36	2.91	2.84	1.79		2.05		2.05		3.15	2.55
Tb								0.90	1.35	1.30	0.78		1.02		1.03		1.55	1.23
Yb								1.81	2.50	2.32	0.94		1.02		1.85		2.86	2.17
Lu								0.21	0.35	0.29	0.13		0.14		0.23		0.36	0.28
Hf								4.90	8.26	7.71	3.00		3.44		4.17		7.98	5.44
Ta								2.09	3.20	3.39	2.04		2.20		2.49		1.04	1.32
Th	2	1	1	1	2	2	1	2.2	2.6	3.2	2.2	1	2.5	4	4.3	1	1.9	2.1

Table 2. Continued

Sample id	57750	57713	57742	57744	59601	59602	57712	BH3A[1]	BH22[1]
Location	Kaas	Sandkås	Kløven	Kløven	Listed dyke	Listed dyke	Sandkås	Gneiss	Granite
Type	3	3	3	3	3	3	4	Basement	Basement
SiO_2	49.89	50.93	51.96	52.46	56.32	54.26	49.81	73.08	73.81
TiO_2	3.80	3.64	3.50	3.58	2.19	2.31	3.23	0.44	0.34
Al_2O_3	16.36	15.31	14.68	14.88	15.81	16.74	13.46	13.27	13.06
FeO^{total}	13.07	12.51	12.58	12.47	9.19	9.62	13.71	2.45	1.82
MnO	0.12	0.15	0.16	0.16	0.21	0.15	0.22	0.06	0.04
MgO	3.23	4.29	4.06	3.85	3.57	3.85	6.01	0.46	0.26
CaO	6.19	6.51	6.36	5.57	5.63	6.45	9.73	1.37	1.23
Na_2O	3.95	3.71	3.50	3.66	4.25	3.98	2.34	2.86	3.16
K_2O	1.97	1.82	2.08	1.96	2.15	1.93	0.74	5.38	5.36
P_2O_5	0.90	0.84	0.87	0.88	0.46	0.44	0.33	0.13	0.07
sum	100.00	100.00	100.00	100.00	100.00	100.00	100.00	99.50	99.15
volatiles	2.87	2.22	1.80	1.57	1.31	1.74	2.31	3.00	4.00
Fe^{2+}/Fe^{total}	0.63	0.78	0.82	0.62	0.78	0.74	0.73	-	-
Mg#	35	43	42	41	46	47	49	7	4
Sc	25	21	18	21	22	21	29	6	4
V	189	178	186	197	151	162	358	14	6
Cr	36	31	35	36	32	31	126	-	-
Co	61	64	57	55	46	54	68	92	73
Ni	53	46	42	41	33	43	98	-	-
Cu	24	20	14	18	6	16	239	-	-
Zn	217	126	153	152	120	110	116	-	-
Ga	25	24	24	23	20	23	24	-	-
Rb	28	29	38	43	49	48	20	199	256
Sr	591	586	539	529	456	559	333	135	103
Y	47.6	42	44	45.8	46.7	40.4	40.8	39	62
Zr	290	278	305	309	304	232	218	297	307
Nb	17.6	17.4	18.4	19.3	15.2	12.1	24.5	14.5	17.0
Ba	756	712	818	781	630	622	173	914	736
La	32.1	30.7	34.8	36.6	35.6	26.3	24.5	51.1	93.9
Ce	80.7	76.9	82.9	83.4	81.3	62.6	61.2	104.0	186.0
Nd	49.6	48.2	54.2	51.9	44.7	38.4	34.7	37.9	62.4
Sm				9.61	8.21				
Eu				3.15	2.39				
Tb				1.64	1.40				
Yb				3.54	3.32				
Lu				0.45	0.46				
Hf				7.33	6.93				
Ta				1.03	0.92				
Th	1	1	1	1.8	3.5	3	1	22	33

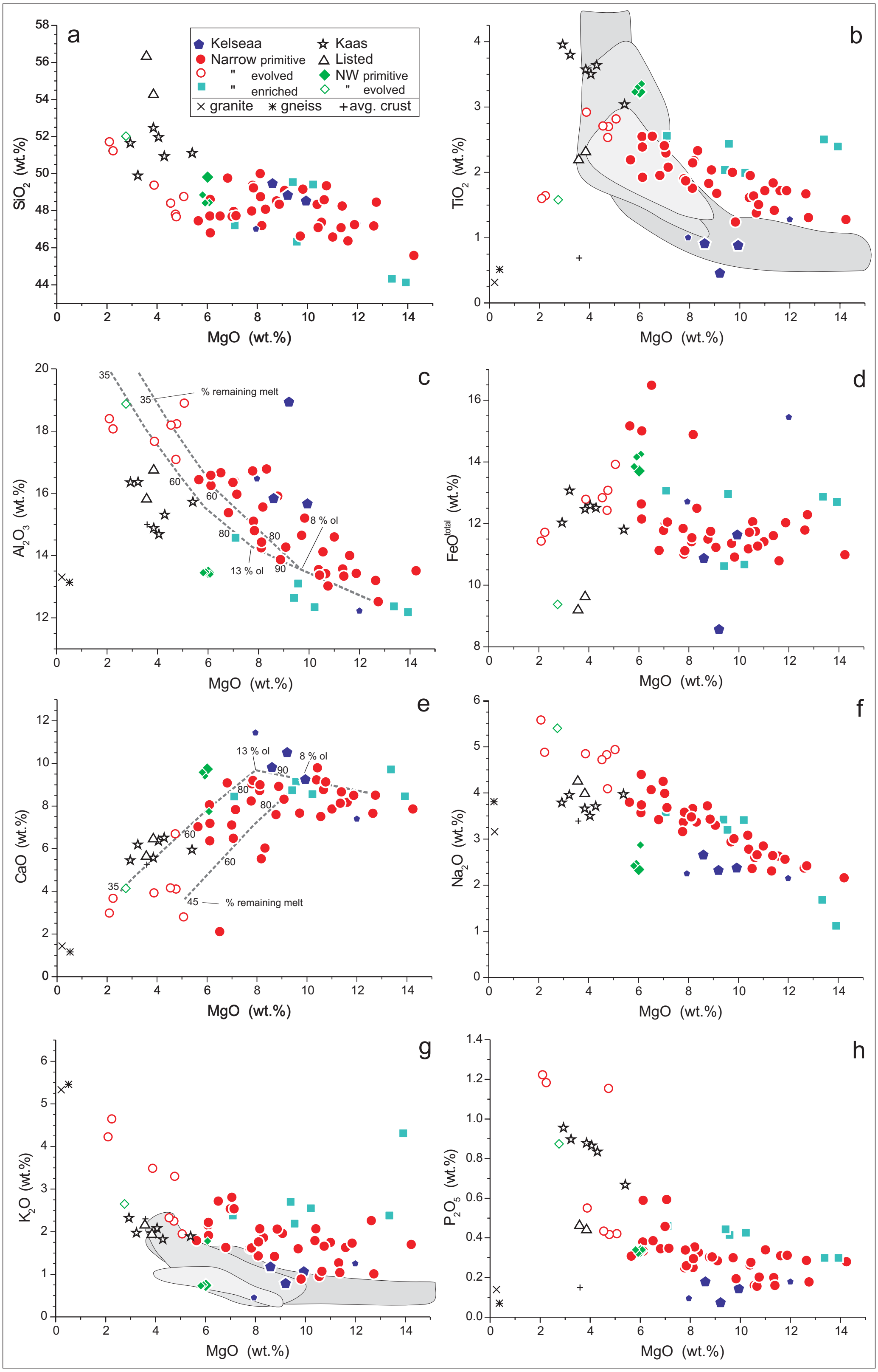

Figure 8: Major element variations for the Bornholm dykes. Symbols as in Fig. 7 except: x: basement gneiss; *: Hammer granite (data: T. E. Waight pers. comm.); +: average middle continental crust (Rudnick and Gao, 2003). In (c) and (e) are shown examples of magmatic evolution modelled by fractional crystallization of sample 59620; see text for details. In (b) and (g) fields for Central Sweden Dolerite Group (pale grey), Protogine Zone Dolerite Group (medium grey) and Blekinge Dalarne Dolerite Group (darkest grey) are shown (Solyom et al., 1992).

Geochemically five main types of mafic dykes can be distinguished on Bornholm. Type 1 (tholeiitic basalts) is represented by three samples from the Kelseaa dyke, a dyke from Stammershalle with strike 42°NE (57719), and a dyke intruded into the Kelseaa dyke.

Type (2) comprises most narrow dykes, and is by far the largest group (46 samples). These are transitional to alkaline, predominantly potassic alkali basalts, trachybasalts and basanites. Type (2*) represents a group of six narrow dykes distinctly more enriched in incompatible elements than other type 2 dykes.

An evolved type (3) consists of samples from the Listed and Kaas dykes, two smaller dykes located not far from the Kaas dyke and probably closely related to it, and two dykes from Kløven south of Kaas. Kaas and related dykes are shoshonites and potassic trachyandesites, and the more sodic Listed dyke samples are mugearites. Samples from the last of the large dykes, the Salne dyke, are all very altered and have largely been left out of this study. This dyke seems to have been a duct for hydrothermal fluids. We note the unusual NE orientation of the Salne dyke that is similar to the Kelseaa dyke.

The WNW- to NW-trending dykes are also geochemically distinct. Type (4) comprises the only quartz tholeiites on Bornholm (Table 1; Obst, 2000). They have relatively low alkali and Al_2O_3 contents and high CaO and TiO_2 for their MgO contents.

Although most of the dykes petrographically appear rather fresh, postmagmatic alteration processes, such as hydrothermal activity, may have disturbed the distribution of, in particular, the more easily mobilized elements K, Rb, Sr, and Ba. However, Ba correlates well with Nb and therefore does not appear to have been significantly mobilized. By contrast, Rb, K, and to a limited extent Sr, show more scatter (not shown). Immobile Zr, though, correlates broadly with K_2O (not shown) and attests that alteration effects are quite limited. We therefore suggest that, although some disturbance has occurred by secondary processes, it has only affected the most mobile elements, and the geochemistry of the dykes is thought to largely reflect magmatic processes. This is despite the fact that less than half of the samples have volatile contents below 3 %, and ten samples have 5 – 10 % volatiles. These elevated volatile contents may partially reflect that the sampled dykes were emplaced as un-degassed magma at considerable depth. Measured $Fe^{2+}/Fe^{total}_{average} = 0.74 \pm 0.07$ (1σ, N = 50, mafic samples only) is typical for alkaline magmas (Middlemost, 1989). The tight normal distribution of this ratio does not indicate large scale secondary oxidation. Low temperature alteration, apparent from petrographic studies, however, is probably the cause of spuriously high values of MnO in nine rocks (MnO = 0.25 – 0.48 %), and occasionally high FeO^{total} values.

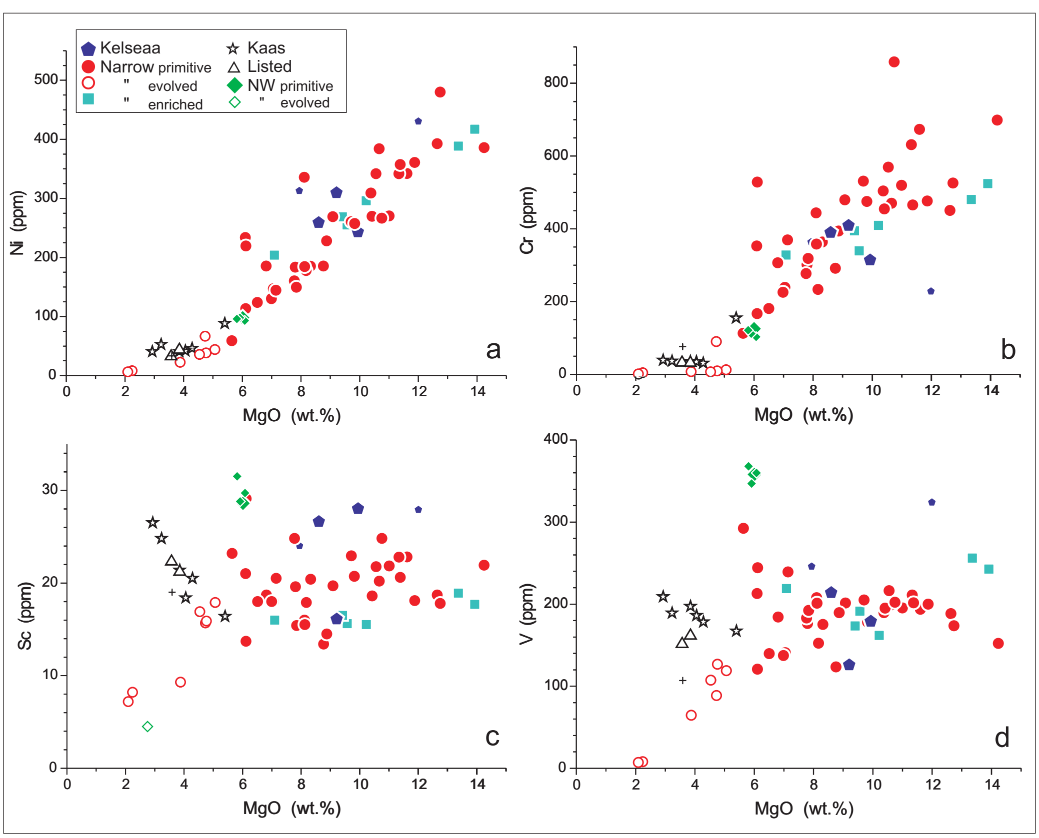

Figure 9: Variation diagrams for selected compatible trace elements vs. MgO. Symbols as in Fig. 8.

Kelseaa-like dykes (type 1)

Three samples from the Kelseaa dyke have been analyzed. They are olivine tholeiites with high MgO contents (8.5 - 12 %), Mg# (0.69 - 0.74), Ni (250 - 430 ppm) and Cr (225 - 400 ppm). SiO_2 concentrations are 47.3 - 49.5 %. The internal geochemical variation in the dyke may reflect differentiation processes during cooling or repeated magma injection in the dyke. Some of the gabbroic rocks in its central part are partial cumulates. The high Al_2O_3 and low FeO^{total} of sample 59635 can be ascribed to the effect of 20 % plagioclase accumulation, although Sr is not high. The concentrations of the incompatible trace elements Rb, Ba, La, Ce, Nd, Y, Zr, and Nb in 59635 are about half of those in 59633. This, together with relatively high Ni and Mg# in 59635, indicates that around 50 % plagioclase and olivine cumulus crystals are present in this rock, which also explains its relatively low V-concentration. Samples 59633 and 59656, from near the dyke margin, are almost identical and may best represent the magma composition. Kelseaa and related magmas have lower TiO_2 (0.5-1.3 %), Sr and Nb than other Bornholm dykes and also have relatively low Na_2O, K_2O, and P_2O_5 (Figs. 8 & 10).

The Kelseaa samples have negative Sr, P, and Ti anomalies in Fig. 11a. Apatite is an early precipitating phase in the Kelseaa dyke (Callisen, 1934), and accu-

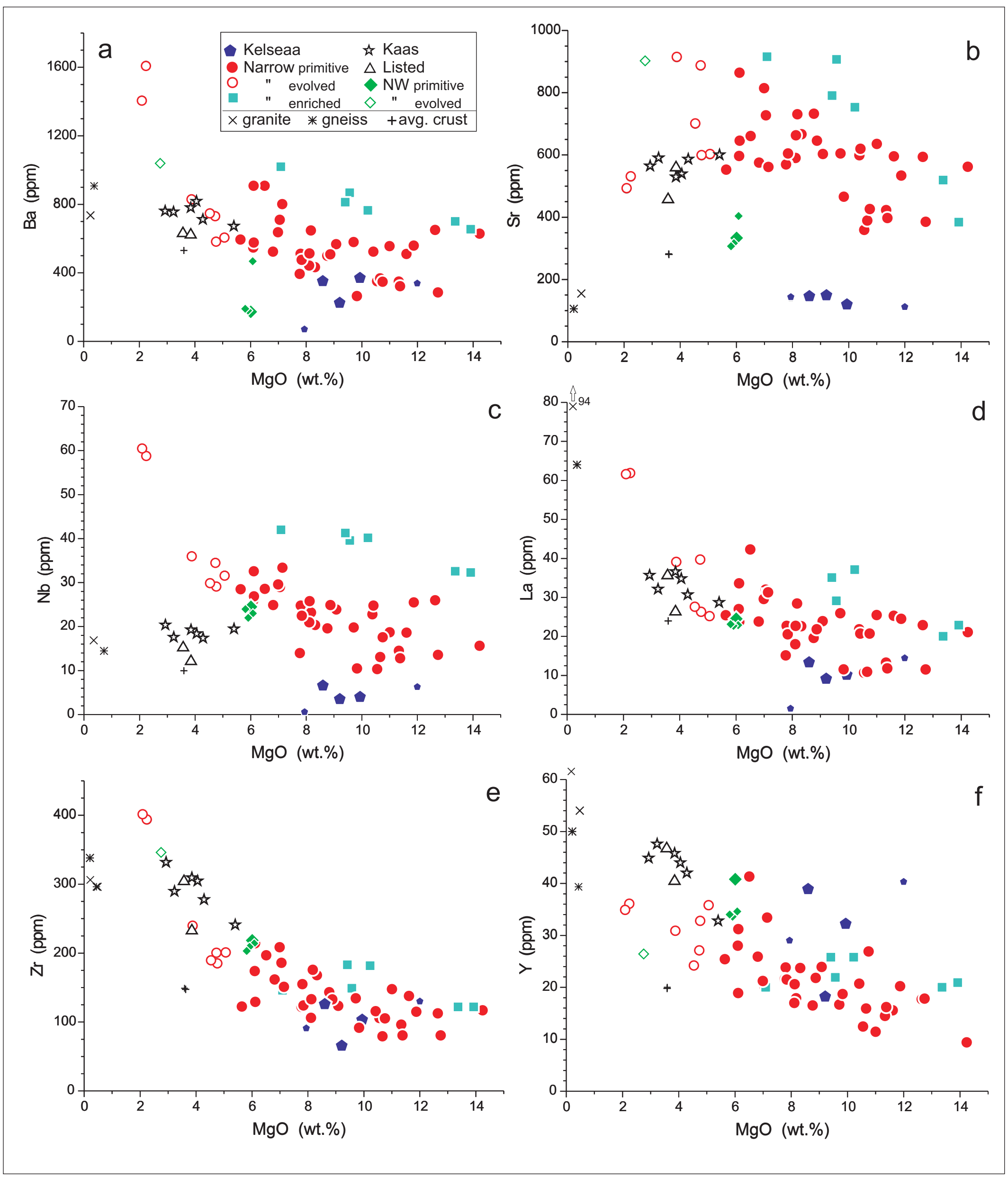

Figure 10: Variation diagrams for selected incompatible trace elements vs. MgO. Symbols as in Fig. 8.

mulation/fractionation of this mineral in the magma chamber could have generated these anomalies, whereas it cannot explain the negative Th anomaly. The heavy REEs are relatively variable having Tb/Yb_N = 1.2-1.8, which indicates an origin by mantle melting at shallow to intermediate depth.

Sample 57719 has very low concentrations of incompatible elements, apart from Rb, Ba, K and Sr (Fig. 11a). The trend is even more depleted than average N-type MORB (Normal-type Mid Ocean Ridge Basalt), but a Tb/Yb_N ratio of 1.8 is higher than in MORB, indicating deeper mantle melting.

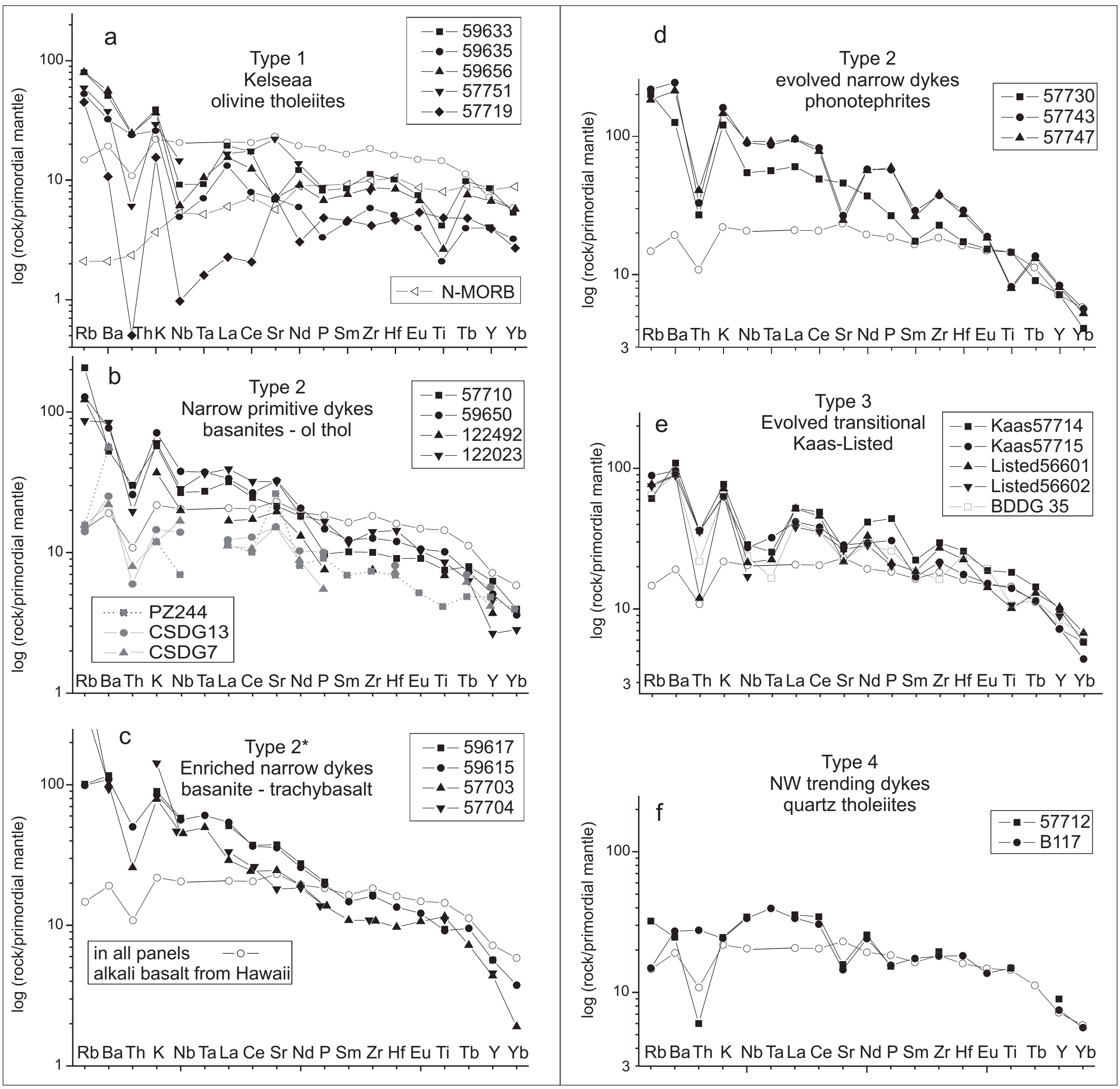

Figure 11: Trace element variation diagrams (spider diagrams) for the mafic dykes. (a) the Kelseaa type; (b) the narrow type with three examples of primitive mid Proterozoic Swedish dykes from the Protogine Zone Dolerite Group (PZDG) and the Central Swedish Dolerite Group (CSDG) (Solyom et al., 1992); (c) most enriched samples of the narrow type; (d) the most evolved narrow dykes: phonotephrites; (e) evolved rocks of the Kaas type and Listed dyke. Also shown is a dyke from the Blekinge Dalarne Dolerite Group (BDDG) which has comparable major element composition (Solyom et al., 1992); (f) NW-trending dyke type. B117 is from Obst (2000). Compositions have been normalized to mantle from Sun & McDonough (1989). An alkali basalt, Honolulu Series, Oahu, Hawaii (sample 65KPO-1, Clague & Frey, 1982) is shown for comparison on all diagrams. (a) also shows an N-type MORB (Hofmann, 1988). Note that the vertical scale differs.

The narrow mafic dykes (type 2) and enriched narrow dykes (type 2*)

The trace element compositions of the narrow dykes are distinctly different from the Kelseaa dyke. The narrow dykes comprise a wide compositional range. They vary in alkalinity from transitional to basanitic, with a few evolved phonotephrites and tephriphonolites. These rocks have very variable MgO contents (2 - 14 %). Among the most magnesian samples three are picrites, and several others have high Cr (> 500 ppm), Ni (> 400 ppm), and Mg# > 65, and may represent near-primary mantle-derived magmas (Table 2, Figs. 8 & 9).

There is a correlation between major element concentrations and petrographic groups. The olivine ± clinopyroxene-phyric samples have primitive compositions with high MgO (> 8 %) and CaO, while the aphyric samples are relatively evolved with MgO < 8 %. The olivine + plagioclase-phyric dykes, which do not include the alkaline dykes, are in many respects intermediate between the other two petrographic groups, although most samples have lower MgO (< 8 %) and CaO, and higher Al_2O_3 than the other two groups.

The narrow dykes have relatively smooth spider diagram patterns except for the LIL (Large Ion Lithophile) elements (Fig 11b). Some of the samples display small positive Sr anomalies. A positive Sr spike is developed in highly magnesian samples that have presumably experienced the least extent of crystal fractionation. Only the most evolved phonotephrites with MgO concentrations of 2.1 and 2.2 % have troughs at Sr, Eu, and Ti. The element patterns therefore do not suggest fractional crystallization of plagioclase until MgO < 4 % during late stages of differentiation. A lack of fractionation-related troughs persists even in samples with low MgO-contents, e.g. samples 59604 (5.64 % MgO, hawaiite) and 57730 (3.88 % MgO, phonotephrite).

Differentiation of the narrow dykes was by fractionation of olivine ± clinopyroxene. The plagioclase phenocrysts in samples with > 4 % MgO are accordingly considered to be related to late stage crystallization of the magmas; plagioclase was not involved in fractionation. Initial crystallization probably took place in a shallow magma chamber, subsequent to some fractionation at greater depths. Constant V-concentrations with decreasing MgO show that Fe-Ti oxides did not fractionate. This also suggests that clinopyroxene was the dominating phase in the extract (K_D,$V^{cpx\text{-}liq}$ = 0.9, (Ulmer, 1989)). Compared to some of the few published primitive compositions from southern and central Sweden (one dyke from the Protogine Zone Dolerite Group and two from the Central Swedish Dolerite Group (Solyom et al., 1992)), the Bornholm dykes are enriched in incompatible elements and show a more fractionated pattern (Fig. 11b), as evident by the generally lower Zr/Nb ratios of 4-10 in type 2 rocks compared to 7-22 in PZDG and CSDG samples.

Phonotephritic magmas are late fractionation products of highly alkaline magmas and relate samples 57730, 57743 and 57747 to the narrow basanitic dykes.

The two most magnesian samples are potassic basanitic picrites (57703 and 57704) with much lower silica than the rest. Four potassic trachybasalts are also particularly K-rich and incompatible element enriched (high also in P_2O_5, Ba, LREE (Light Rare Earth Elements), Zr, and Nb), but less SiO_2-depleted, and low in Al_2O_3 (Fig. 8 & 10, Tables 1 & 2), as is also apparent in the spider diagram (Fig. 11c). These 6 samples will be treated separately as subtype 2* in the discussion.

The Kaas, Kaas-like and Listed dykes (type 3)

This group of evolved rocks is transitional to slightly quartz normative and potassic. The more sodic Listed samples deviate in most diagrams from the trends defined by the Kaas dyke and the Kaas-like dykes. Mineralogical variations across the Kaas and Listed dykes have been described in detail by Jensen (1966).

The 40 m wide Kaas dyke displays some internal variation. Sample 57715 has higher MgO, Ni, Cr and Sc and lower SiO2 than 57714. This may be caused either by in situ fractionation or (not evident in the field) by multiple injection. Two dykes from Kløven (57742 and 57744), one from Sandkås (57713) and one close to the Kaas dyke (57750) have Kaas-like compositions that distinguish them from evolved type 2 dykes, and include relatively high TiO2, P2O5, and V (Figs. 8 & 9).

The Listed dyke has higher SiO_2 contents (54.3-56.3 %) than the Kaas-like dykes (49.9-52.5 %), and lower concentrations of FeO^{total}, TiO_2, and P_2O_5. The two samples from the 30 m-wide Listed dyke (59601 and 59602) are from the contact and center of the dyke, respectively, and show a small, systematic difference indicating that some differentiation took place between injection of the outer and inner parts of the dyke, as is also implied by their different feldspar phenocryst assemblages.

The spider diagram patterns of the evolved dykes (Fig. 11d) are in many respects similar to that of the Kelseaa dyke, the difference being mainly a higher degree of enrichment of LREEs and HFSEs (High Field Strength Elements) in the evolved type 2 dykes. Concentrations of the LIL elements are only slightly higher than in Kelseaa. Concentrations of heavy rare earth elements are similar, although the HREE are slightly more fractionated (Tb/Yb_N = 1.8-2.4) than in the Kelseaa dyke, and therefore indicate a deeper melt extraction. Some Blekinge Dalarne Dolerite Group (BDDG) rocks resemble the type 3 dykes (Fig. 11d).

NW-trending dykes (type 4)

The Sandkås sample 57712 (strike: 110°), as well as three other samples from northern Bornholm (Obst, 2000), and a trachytic (kullaite) dyke from central Bornholm (Jensen, 1988), have trends between WNW and NW. Sample 57712 is very similar in composition to those reported by Obst (2000). These are distinct from other Bornholm dykes in having lower Al_2O_3, Na_2O, K_2O and higher Sc, V and Cu (Figs. 8-10). Together with the more evolved Listed and Kaas-type dykes the NW-dykes are the only quartz normative examples on Bornholm. The incompatible element patterns of these rocks show less enrichment in very incompatible elements than type 2 rocks, and they have negative Sr anomalies (Fig. 11e).

Discussion

Geochronology

Both field relations and palaeomagnetic studies suggest that the dykes were intruded in four or five episodes between the formation of the younger granites (c. 1.45 Ga, Zariņš & Johansson, 2008) and the Permian (Münther, 1945a; Abrahamsen, 1977; Abrahamsen et al., 1995; Lewandowski & Abrahamsen, 2003). These four events at c. 1326 Ma, c. 1220 Ma, 950-900 Ma and ≈300 Ma can be correlated to the Kelseaa dyke, the narrow dykes, the Kaas dyke, and the-NW trending dykes, respectively. The Listed dyke has been suggested to be somewhat younger than the Kaas dyke (700 – 800 Ma, Abrahamsen, 1977), and may accordingly represent a separate intrusive episode. As its age is uncertain, however, and because the Listed dyke has compositional affinities to the Kaas-like dykes, we group them together. The geochemistry of the dykes indicates that (a) the Kelseaa, (b) the narrow dykes, (c) the evolved Kaas and Listed dykes and (d) the NW-trending dykes define four distinct compositional types (types 1-4) which is in accord with the above sequence of intrusion. In the following we will discuss the geochemistry of the dykes based on the hypothesis that each intrusive event represents a distinct episode of mafic magmatism.

Fractional crystallisation

Kelseaa (type 1). The variation among the Kelseaa dyke samples in terms of major elements suggests multiple intrusion in the dyke. This has not been substantiated by field evidence, possibly due to poor exposure. Although petrographic observations suggest differentiation during solidification, the compositions of the samples cannot be related by simple fractionation processes. The geochemistry suggests that magmas of variable and independent derivation were involved. *Narrow dykes (type 2).* These make up rather well defined trends in the variation diagrams (Figs. 8-10) and are here considered as products of similar crystallization histories of a range of primitive magmas. Overall initial fractionation of olivine +/- chromite is indicated for magmas with > 9 % MgO by the decrease with MgO of only Ni, Co, and Cr (Fig. 9), and the increase of several other elements not present in olivine, e.g. Na_2O and Zr (Figs. 8 & 10). Clinopyroxene + olivine fractionation is indicated as the melts evolved through 9-8 % MgO by decreases in CaO, SiO_2, and Sc, together with the continued decrease of Ni and a more pronounced increase of excluded elements such as TiO_2, Al_2O_3, Na_2O, K_2O, and P_2O_5. Clinopyroxene and olivine are joined by Fe-Ti oxide fractionation very late in the magmatic development for the few samples with MgO < 5.6 %, as shown by strong decreases in FeO, TiO_2 and V (Figs. 8 & 9). Plagioclase and apatite are not significant fractionating phases since Na_2O, P_2O_5, LREEs, and Sr increase into the most evolved samples (Figs. 8 & 10). The late onset of feldspar crystallization is typical for highly silica undersaturated (basanitic and nephelinitic) magmas that fractionate towards phonolitic compositions (e.g. Holm et al., 2006).

The simple fractionation scheme that encompasses the majority of the narrow dyke magmas was modelled quantitatively from a starting melt compostition using picrite sample 59620 as an example (Fig. 8c, e). This sample may have accumulated some olivine (the sole phenocryst phase) but correction for this would not be well constrained and would only change the modelling very slightly as regards the amount of crystallization involved. Equilibrium olivine and clinopyroxene were calculated for each fractionation increment of 1 %. The model shows that after initial fractionation of 8-13 % olivine, clinopyroxene started to crystallize and the cotectic proportions are indicated to have been around 1 ol:5 cpx. Most samples are described by < 20 % fractionation. The interval 13 - 6 % MgO is covered by c. 40 % fractionation. The most evolved phonotephrite compositions can be modelled as samples with 35-45 % residual melt (Fig. 8c, e).

Kaas-Listed (type 3). These rocks have high concentrations of Sc as well as TiO_2 and P_2O_5, which show well-defined negative correlations with MgO (Figs. 8 & 9), implying that neither clinopyroxene, Fe-Ti oxides nor apatite fractionated in significant amounts from these magmas over the restricted compositional range sampled. Negative Sr anomalies in the spider diagram (Fig. 11d) suggest that plagioclase fractionated in the precursory magmas. Low Ni, together with low MgO in these rocks, indicate that olivine was also important in the fractionate. Because some BDDG rocks resemble the Kaas-Listed dykes we have used a primitive BDDG sample (#56) with 11.4 % MgO and 49.9 % SiO_2 (Solyom et al., 1992) as the parental composition for fractionation modelling. This shows that Kaas-like type 3 magmas with 4 % MgO may result from 53 % crystal extraction of 11 % olivine (covering the range 11.4 to 7.0 % MgO) followed by 29 % plagioclase + 11 % olivine + 0.5 % clinopyroxene + 0.1 % Fe-Ti oxide (7.0 to 4.0 % MgO). It is noted that Kaas-like samples have twice the TiO_2 and P_2O_5 concentrations of the Listed samples and their parental magmas were therefore probably much more enriched. Moreover, as seen from the SiO_2- and TiO_2-contents, the Listed and Kaas magmas also evolved differently, possibly because their magma chambers were emplaced at different depths.

Compositional considerations indicate that the evolved type 3 dykes had a different parental magma type from the Kelseaa (type 1). The Kelseaa dyke has higher CaO but lower Sr-concentrations than the evolved dykes, which is not compatible with derivation of the latter by fractionation of plagioclase and olivine from a magma geochemically similar to type 1. Furthermore, petrographic observation of the Kelseaa dyke suggests that apatite was an early crystallizing phase, in contrast to the differentiation history of the evolved dykes.

NW-trending dykes (type 4). The medium-K basalts of the NW-trending dykes show very little variation. These rocks are quite evolved with Mg# around 49. The slightly silica undersaturated Bjergebakke mugearite (Table 7 in Jensen, 1988) would be difficult to derive from these highly hypersthene normative basalts by fractional crystallization, and they are not likely to be comagmatic.

Contamination

Contamination of mafic magmas commonly takes place in crustal magma chambers accompanying fractional crystallization. For three of the dyke types discussed, Kelseaa, Kaas-Listed and the NW-trending dykes, quantitative modelling of possible contamination is not feasible because only a very restricted compositional range is available. Instead the effects of adding crustal material to mantle melts are considered on the basis of element ratios that typically have a significant contrast between continental crust and mantle melts. Ratios such as Ba/Nb and La/Nb are sensitive to contamination with crust-derived material which typically has high Ba, LREE, and low Nb, as exemplified by the Bornholm gneiss and a Hammer granite (Table 2), compared to mantle melts, exemplified by oceanic basalts (Fig. 12). Moreover, these ratios do not change significantly during fractionation of the observed mineral assemblages.

Kelseaa (type 1) and Kaas-Listed (type 3) dykes. The

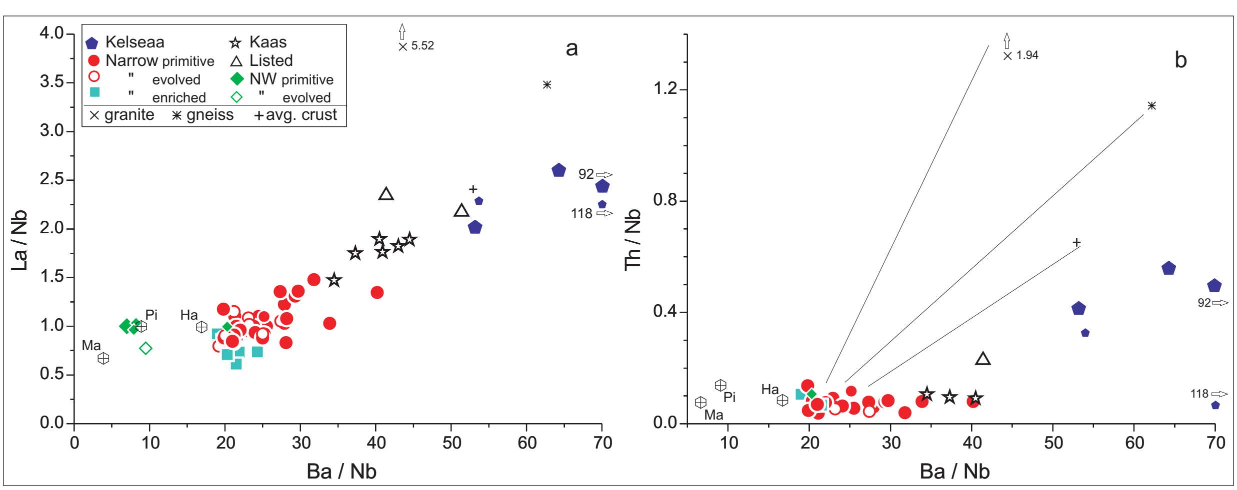

Figure 12: (a) La/Nb versus Ba/Nb; (b) Th/Nb versus Ba/Nb. Examples of OIB hot spot magmas are shown as hexagons with plus: Ha –Hawaii (same as in Fig.9); Ma – Mangaia HIMU-type OIB, sample M13 (Woodhead, 1996); Pi – Pitcairn Island EM1-type OIB, sample Pit89-1 (Eisele et al., 2002). (b) includes mixing trajectories between low Ba/Nb dykes and various crustal compositions. The trend of Kelseaa type and Kaas-Listed type dykes towards high Ba/Nb and La/Nb seems unrelated to assimilation of local basement compositions. See text for discussion. Other symbols as in Fig. 8.

Kelseaa (type 1) dykes consistently have the highest values of both Ba/Nb (54-111) and La/Nb (2.0-2.6) (Fig. 12), whereas the Kaas-Listed dykes have ratios (33-45, 1.4-2.0, respectively) intermediate between Kelseaa and the narrow dykes (Ba/Nb = 19-32, except for a few outliers). The Kelseaa dykes are also enriched in Rb, Ba, Th and K that are usually high in felsic crustal rocks, and we conclude that significant crustal contamination of the magmas has taken place. Sample 57719 is relatively enriched in the fluid-mobile elements Rb, Ba, K, and Sr. This, and the very high Ba/Th ratio of 1700, suggest that the N-MORB pattern was modified by addition of a fluid-borne agent, which may also have influenced sample 57751 (type 2). The Kaas-Listed magmas seem somewhat less contaminated.

The Kaas-Listed magmas cannot have developed from magma similar to the Kelseaa dyke by means of AFC (assimilation coupled with fractional crystallization) processes because they have lower Ba/Nb but much higher Ba-concentrations, and alkali feldspar is not considered a possible liquidus phase. The Kaas-Listed dykes evolved from magmas more Nb-enriched than the Kelseaa magmas, if it is accepted that the geochemistry of the Kelseaa samples mainly reflects a melt composition rather than a cumulate, as it was argued at least for sample 59656.

The Listed samples have higher La/Nb and Ba/Nb than the Kaas and Kaas-like dykes and may be more contaminated. It is noted, however, that the enrichment in Ba and LREE is not accompanied by Th enrichment (Fig. 12b). The difference between the two Listed samples may be caused by multiple injection, as indicated petrographically, of variably contaminated magmas.

Specific contaminants for the dykes may be the exposed crustal rocks. These may be approximated by the grey granitic gneiss and Hammer granite (the northernmost younger granite, Fig. 1, Table 2). In Fig. 12b we also show the composition of these and a global average of middle continental crust (Rudnick & Gao 2003). Because only amphibolite facies gneisses are exposed (Callisen, 1934), upper crustal rocks are not common below the present exposure level and are probably not relevant for discussion of the Bornholm dykes, since contamination would have involved the middle or lower crustal rocks. Mixing of two components in this type of diagram will produce straight lines (Fig 12b). Type 1, 2 and 3 samples are situated on a broad trend in Fig. 12a, which includes the crustal average but not the local basement. If an average type middle crust was assimilated by the Kelseaa and Kaas-Listed magmas, very high proportions are indicated for Kaas-Listed, whereas the Kelseaa samples exceed crustal values. Assimilation of the local basement with high La/Ba ratio is only indicated for one sample of the Listed dyke that lies above the main trend in Fig. 12a. Either crustal contamination is not generally related to the locally exposed basement, or a different process caused the high Ba/Nb and La/Nb ratios in type 1 and 3 magmas.

The narrow dykes (type 2). The variation of the narrow dykes does not indicate much local continental crustal assimilation as they have Ba/Nb and La/Nb ratios close to those of mantle rocks and oceanic basalts (Fig. 12). Ba, Th and Nb were all very incompatible in the dyke magmas. The variation of ratios of these elements in type 2 dykes is not towards the crustal rocks, as demonstrated in particular by the constant and mantle-like Th/Nb ratio (Sun & McDonough, 1995). Sr is also incompatible in most type 2 magmas, and the correlation of ratios Ba/Nb and Sr/Th with Sr/Nb does not appear to be related to assimilation of relatively evolved crust (with high Th and low Sr), but

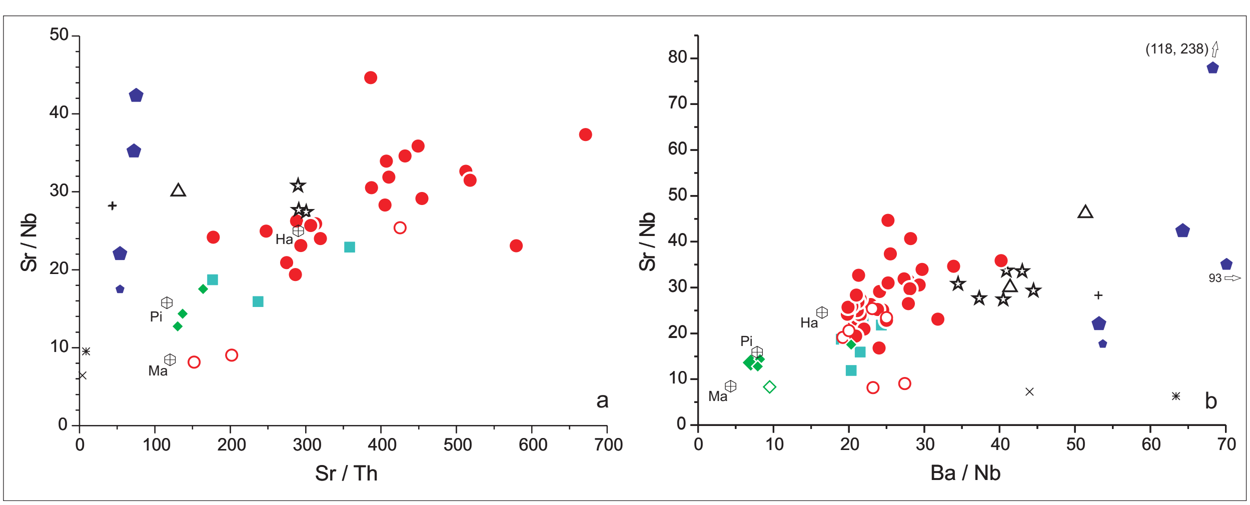

Figure 13: (a) Sr/Nb versus Sr/Th; (b) Sr/Nb versus Ba/Nb. Symbols as in Fig. 12. Sample 57719 is not shown in (a) due to extremely high and uncertain Sr/Th due to Th concentration close to the detection limit (Table 2).

rather some agent rich in Ba, Sr, and LREEs (Figs. 12 & 13). The rocks enriched in Sr, Ba, and La have both a small negative Nb-anomaly and a positive Sr-anomaly in spider diagrams (Fig. 11b). These are the type 2 rocks with the highest Zr/Nb (= 6 - 10). There is no relation between any of these ratios and degree of magmatic differentiation, and modification of type 2 melts with relatively low Zr/Nb (4-6) was therefore not by assimilation and fractionation processes involving crust that typically has high Zr/Nb. HFSE ratios are generally not thought to be affected by post magmatic processes. It therefore seems that the elevated Zr/Nb ratios must have been acquired in the mantle.

Mantle melting and source compositions

The folowing discussion of melt generation is mainly based on the modelling in Figs. 14 & 15. Fig. 16 is an attempt to graphically illustrate the models with simplified sketches.

Kelseaa (type 1)

Significant fractionation of the heavy rare earth elements, such as Tb and Yb, in basaltic magmas can only be accomplished by melt-garnet interaction. Three samples of the Kelseaa dyke have Tb/Yb_N = 1.2 - 1.8 (Fig. 14a). A Tb/Yb_N ratio of 1.2 is in accordance with melting in the spinel stability field (see below), whereas the higher ratio of 1.8 requires the presence of garnet in the source. This is an additional indication of the presence of two magmas in the Kelseaa dyke, and it requires the Kelseaa melts to be variably derived over a depth range.

REE-modelling of melting of mantle peridotite in the garnet and spinel stability fields is shown in Fig. 14a. The melts are modelled by aggregated non-modal batch melting. A mantle source (termed DPM) somewhat depleted relative to primitive mantle (McDonough & Sun, 1995) was used. Its composition was calculated as depleted mantle, DM (McKenzie & O'Nions, 1991), enriched by 5 % partial melts generated by 0.5 % melting of a depleted garnet peridote (Tainton & McKenzie, 1994). Such a source can account for the samples with the highest Tb/Yb_N ratios on Bornholm. The Kelseaa samples 59656 and 59635 with Tb/Yb_N = 1.2 – 1.3 fall below the model curve and must have been generated from a source more depleted than that of the model. A depleted type mantle is also inferred from the geochemistry of the Kelseaa dyke in general with Nb_N and $MREE_N$ < 10 (Middle Rare Earth Element), and low TiO_2 < c. 1 % giving a flat trace element spectrum, apart from the enrichment in LILE and LREE (Fig. 11).

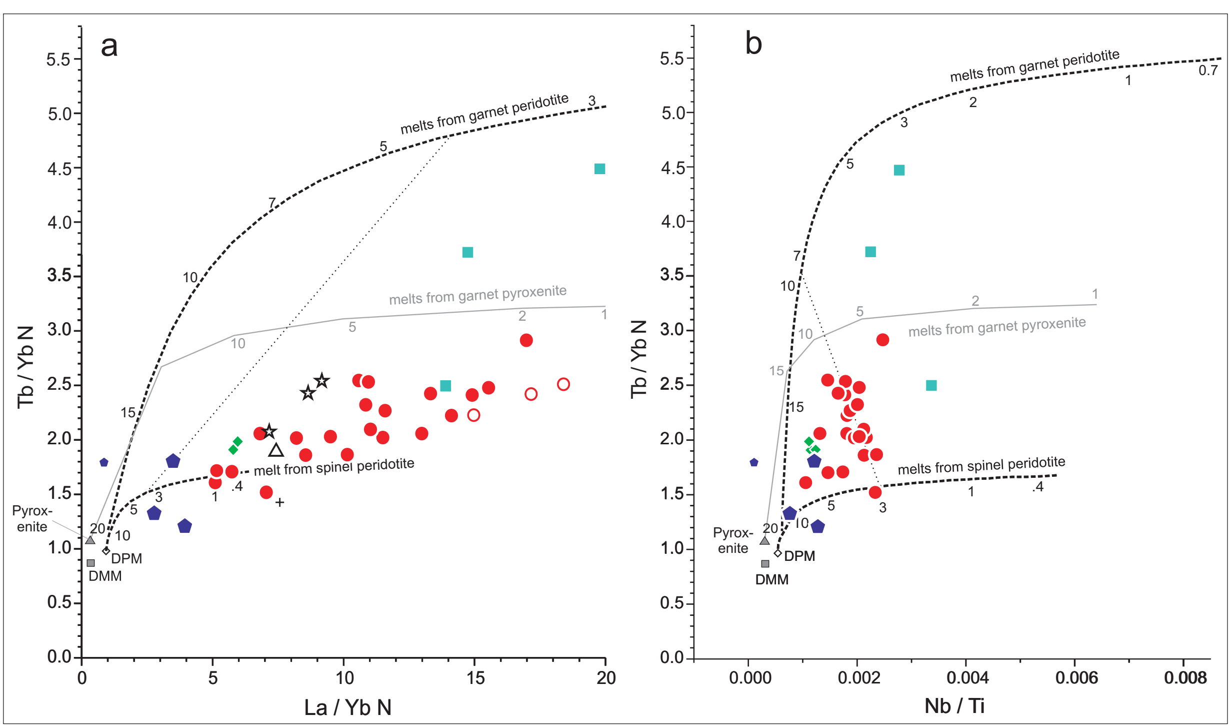

Figure 14: (a) Tb/Yb_N vs. La/Yb_N. (b) Tb/Yb_N vs Nb/Ti. Modelling of melting of a hypothetical mantle source in the spinel peridotite and garnet peridotite stability fields, respectively. Sources are: DMM – depleted MORB mantle; Pyroxenite is recycled MORB mantle, and DPM (mantle somewhat depleted relative to primordial mantle). See text for explanation. La/Yb and Tb/Yb are normalized to chondrite (Anders & Grevesse, 1989). Only primitive samples are shown in (b). Symbols as in Fig. 7.

Depleted sample 57719 with very low La/Yb_N = 0.85 has rather high Tb/Yb_N = 1.8 and it must have been generated at high pressures from garnet-bearing mantle (Fig. 14). The high $Fe_2O_3^{total}$ compared to MORB is also an indication of relatively deep extraction (Klein & Langmuir, 1987).

Sample 59633 with high Tb/Yb_N = 1.8 and La/Yb_N = 3.5 could be generated from the model source by mixing of partial melts from the garnet and spinel stability fields, or by melting during decompression of rising mantle through the garnet-spinel transition. Mixing of melts generated by around 4 % melting would be mixed in the ratio 1 garnet peridotite:12 spinel peridotite. With a more depleted mantle source, a larger proportion of the magma would stem from garnet-bearing mantle. There are no other significant geochemical differences between the Kelseaa samples with higher and lower Tb/Yb, and one depleted source is inferred for them all.

The Bornholm lithosphere at the time of the Kelseaa intrusion was 300 Ma old and thus would be expected to be more than 100 km thick even though it was strongly modified at 1.45 Ga during formation of the granitic crust. Thus, as melting to a large extent took place in the spinel stability field at depths less than 75-90 km, the source must have been located in, but not restricted to, the lithospheric mantle or, alternatively, the lithosphere had been thinned at the time of melt generation. With the apparently unique occurrence of the Kelseaa type a hotspot is hardly indicated, and general heating of the lithosphere would also be expected to yield more magmas. Furthermore, the quite depleted mantle source for the Kelseaa dyke infers melting by decompression, because refractory lithospheric mantle is less likely to melt by conductive heating.

The ultimate source of the Kelseaa dyke, however, cannot have been depleted mantle of the same type as inferred to generate mid-ocean ridge basalts. Although Zr/Nb in the Kelseaa samples is high (20-26) (Fig. 11, Table 2), it is still slightly lower than in typical N-MORB (> c. 30) (Hofmann, 1988). Crustal contamination would not tend to decrease this ratio. Using Nb/Ti as a parameter for the degree of melting (see explanation below for type 2 modelling), the model indicates a relatively high degree of melting (5-10 %) (Fig. 14b), so it is clear that a mantle source that is slightly more enriched than that of N-MORB is required. Incompatible element depleted sample 57719 (believed to represent a melt composition) with its high Zr/Nb = 142 and Th, Nb and LREE-depletion is an indication that MORB asthenosphere was involved in the formation of the Kelseaa (type 1) magmas.

We propose a back-arc extensional regime for these magmas. This may allow MORB-like magmas to be derived in a rifting continental setting. A back-arc setting would also explain the enrichment in fluid-mobile elements and in Th, as discussed above. The very limited amount of magmatism, however, suggests that this extensional process did not progress far.

The narrow dykes (type 2)

The narrow dykes have a wide range of Tb/Yb_N of 1.5-2.9 (enriched subtype 2* has up to 4.5) and a large group of samples form a general trend ranging to Tb/Yb_N = 2.5 and La/Yb_N to 17 (Fig. 14a), suggesting that melting took place across the garnet-spinel stability boundary and, for most dykes, a considerable component was derived in the garnet stability field. These primitive magmas therefore likely formed below the Bornholm lithosphere, either from relatively hot mantle, or from mantle with a relatively low solidus temperature such as other lithologies than peridotite, e.g. pyroxenite, or from hydrous mantle. Extension and lithospheric thinning, as indicated by the preferred dyke orientation, might have assisted the melting, but residual garnet is still required and thus rather deep melting at > 80 km.

Very high La/Yb_N (up to 17) at the high Tb/Yb-end of the main trend would point to very small degrees of melting (below 1 %) of garnet peridotite, whereas the other end of the trend would indicate c. 1 % spinel source melting (Fig. 14a). However, bearing in mind that some of these rocks are preferentially enriched in Ba, Sr, and LREEs, the La/Yb ratios may not only be related to melting of a homogeneous source, and the derived melting proportions may therefore be invalid.

In an attempt to circumvent this problem we have modelled melting using Nb/Ti, which is also a ratio of a highly to intermediately incompatible element. Because both are HFSEs this ratio would not be significantly influenced by the variable enrichment, which is dominated by LILEs and LREEs. The resulting melting curves (Fig. 14b) are broadly similar to those in Fig. 14a. However, a negative trend for type 2 magmas is evident, suggesting much larger degrees of melting: 3 % in the spinel field and around 10 % in the garnet field. If one common source is assumed, then a decrease in the amount of melting with declining pressure requires a lowering of temperature for decompression melting. Only a small temperature change is expected for asthenospheric processes which are mainly adiabatic. Alternatively, the melts could have been generated from two sources with different Nb/Ti ratios and different solidus temperatures and different degrees of melting would be expected at the same temperature.

If a source composed of peridotite with pyroxenite veins rises, the pyroxenite has the lower solidus temperature, and therefore starts to melt at deeper levels (Stracke & Bourdon, 2009). At a given potential mantle temperature, pyroxenite will melt to a higher degree than peridotite. Results of batch melting of pyroxenite can be compared to the peridotite melting already discussed (Fig. 14). As is apparent in Fig. 14b, unrealistically small degrees of melting are modelled at low pressure, whereas garnet pyroxenite melting may be a viable alternative to peridotite. A mixed source, then, would allow for the two lithologies to have have different Nb/Ti ratios and could explain a higher degree (c. 7 %) of garnet pyroxenite melting and a lower degree (c. 3 %) of melting of spinel peridotite, and would not require a variation in source temperature. From Zr-Nb modelling (Fig. 15a) rather similar degrees of melting are suggested: 2 – 3 % for the low Zr/Nb samples which have low Tb/Yb, and around 5 % for the high Zr/Nb (6 – 10) samples.

The narrow dykes reflect a mantle composition which has certain similarities to the source of some ocean island basalts. The dykes with low La/Nb (0.8 - 1.2), Zr/Nb (4 - 6) and Ba/Nb (19 - 26) (Figs. 12, 15) are comparable to young oceanic islands like St Helena, Tubuaii, and Pitcairn Island (e.g. Weaver et al., 1987, 1991; Palacz & Saunders, 1986; Dupuy et al., 1988; Eisele et al., 2002) which represent mantle end members (Zindler & Hart, 1986). These mantle end members have been interpreted to represent recycled oceanic lithosphere which, after subduction, have contributed to OIB (Ocean Island Basalt) melts as parts of rising mantle plumes. The dykes from Bornholm include, however, samples more enriched in LIL elements relative to HFSE and LREE than most oceanic basalts. This is particularly evident in those dykes with La/Nb = 1.2 – 1.6 which also have high Ba/Nb = 30-41, and in those with positive Sr anomalies (Fig. 11b). Thus, if the low LREE/HFSE ratios of the source are derived from typical OIB mantle, the LILE enrichment must have been added from other sources available at the same time, sources which were demonstrated above not to be derived from the crust.

Most type 2 rocks form a well-defined trend that suggests mixing of two distinct end-member compositions (Figs. 12a, 13, 14, 15b). One has high La/Nb, Ba/Nb, Sr/Nb, Sr/Th, Zr/Nb, and Sr/Nd = c. 30. The other end-member has much lower Sr/Nd = c. 16, which is typical for MORB and some OIB (Hofmann, 1997). The high Sr/Nd end-member is suggested to be recycled gabbroic oceanic crust enriched in Sr by plagioclase accumulation. Such a component has also been suggested to be part of some mantle plumes (e.g. Chauvel & Hémond 2000; Kokfelt et al. 2006). This end-member is identical to the type 2 dyke component with relatively high Tb/Yb and low Nb/Ti identified above, which was characterized by a relatively low solidus temperature, as expected from a gabbroic composition.

Because the more enriched subtype 2* dykes that have even more extreme OIB signatures (Zr/Nb = 3 - 4, La/Nb = 0.6 - 0.9, Ba/Nb = 20 - 25) also have higher Tb/Yb_N = 2.5 - 4.5 they were generated at greater depth. These dykes extend from type 2 towards higher Nb/Ti and compositions derived by c. 2 % melting of garnet peridotite (Fig. 14b). Along with incompatible element ratios (Figs. 12 &13) and the lack of a positive Sr anomaly this demonstrates that they had a different source than the predominant type 2 magmas. The apparently small scale of this igneous activity indicates that no major rifting is associated, and melting seems to have taken place under a more or less intact continental lithosphere. Therefore, the

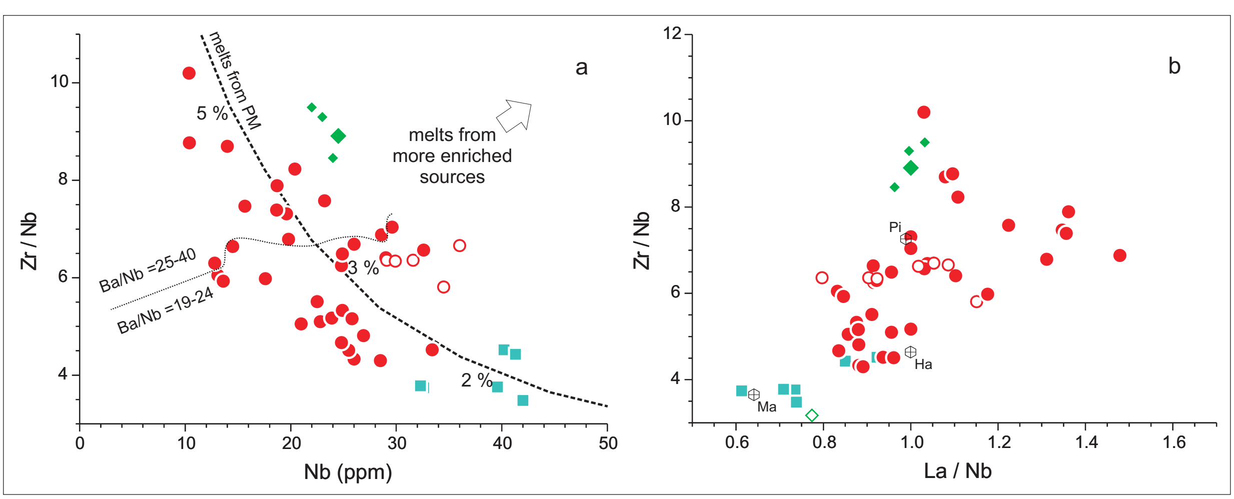

Figure 15: (a) Zr/Nb vs Nb. (b) Zr/Nb vs. La/Nb. In (a): curve for melts from aggregated incremental batch melting of PM (= primordial mantle; Sun & McDonough, 1995) is shown for reference. Thin dotted line separates samples with Ba/Nb higher and lower than 25. Symbols as in Fig. 12. See text for discussion.

most likely cause for magma generation was the presence of extraordinarily hot mantle under Bornholm at this time, and a different event than that which generated type 2 magmatism may be indicated.

Contemporaneous Protogine Zone magmas have a different geochemistry from type 2 magmas and may well have been generated differently. A rifting event at this time in southern Sweden that did not extend to Bornholm, based on the relatively low dyke intensity, may have led to lithospheric thinning and been the trigger for melting in abnormally hot mantle with a composition different from MORB-source asthenosphere, and a plume source under Bornholm may be indicated.

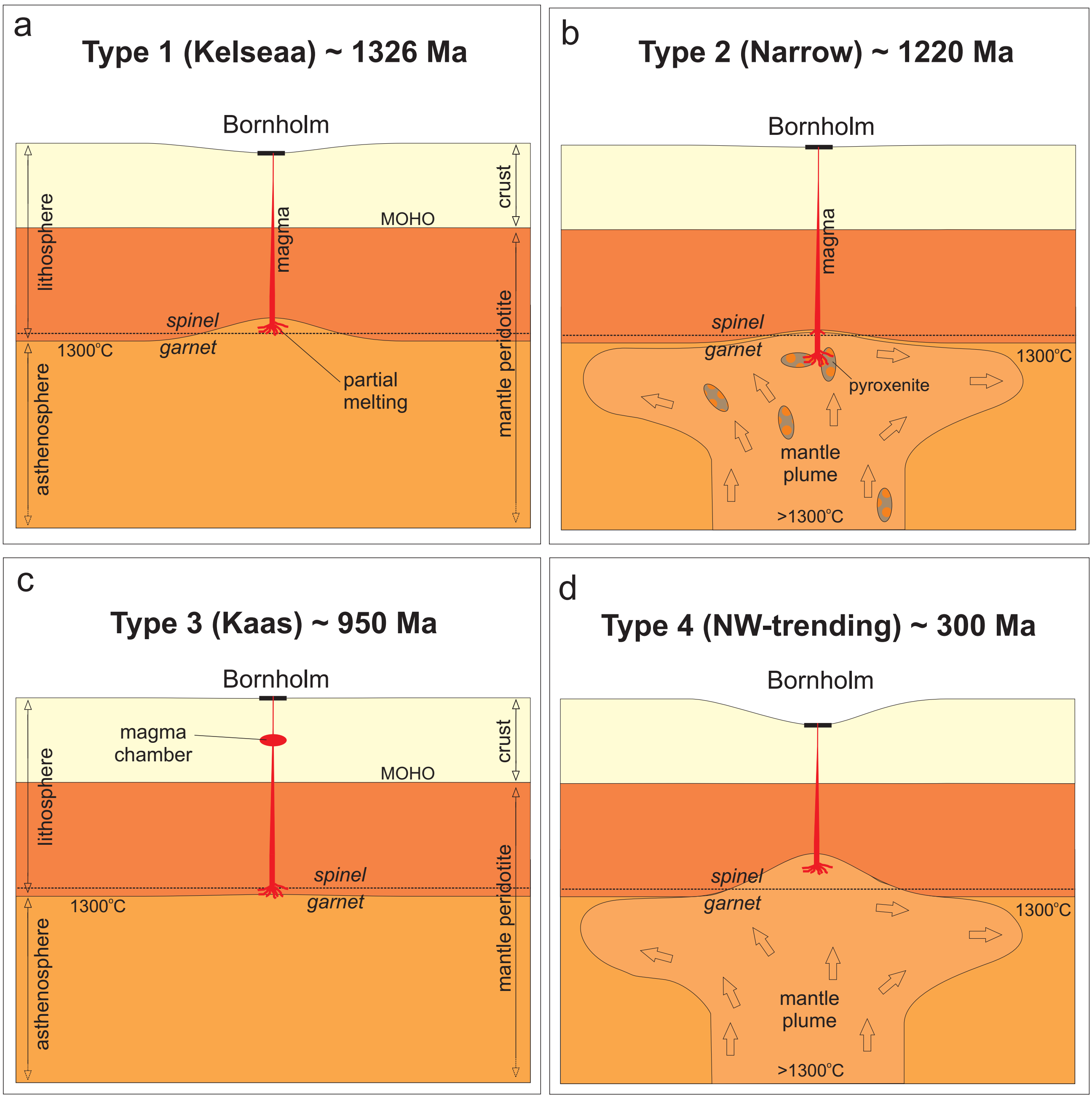

Figure 16: Simplified schematic models for the melting regime for Bornholm mafic magmas. a) Melting mainly of depleted asthenospheric peridotite in the spinel stability field at c. 1326 Ma probably during an extensional tectonic environment in the lithosphere; b) melting of an abnormally hot (> 1300°C) pyroxenitic and peridotitic mantle plume mainly in the garnet stability field at c. 1220 Ma; c) melting of both garnet and spinel peridotite around 950 Ma; d) melting of enriched spinel peridotite probably in a mantle plume under a dilated lithosphere at c. 300 Ma. MOHO is the Mohorovic crust-mantle discontinuity; the 1300°C isotherm is used as the transition between lithospheric and asthenospheric mantle; the depth of the spinel-garnet transition is located at 70-90 km depending on the local temperature gradient.

Kaas and Listed (type 3)

The geochemistry of the evolved type 3 magmas is far removed from precursory mantle melts and may hold no clear indication of their origin. However, the HREE ratios would be expected to be relatively less changed during crustal residence in a magma chamber than more incompatible elements. From the appearance in Fig. 14a these magmas may have originated in a mantle source with a considerable proportion of melts derived from the garnet stability field. Because of their evolved and contaminated nature it is not possible to constrain the possible mantle source(s) further.

NW-trending dykes (type 4)

The Permian dykes seem to have been derived at somewhat shallower depths than type 2 magmas, $Tb/Yb_N < 2$ (Fig. 14), and by slightly larger degrees of melting, provided they had a similar mantle source. This is also suggested by their quartz normative nature and from Zr-Nb modelling (Fig. 15a). Significant lithospheric thinning probably took place at this time. Type 4 magmas were generated from a source with low Ba/Nb (< 10) and more enriched in HFSE than that of other Bornholm magmas, and comparable to the source of several hot spots (Figs. 11, 12, 13, 15). Together with the rather shallow, and high degree of melting indicated from REEs (Fig. 14), this strongly suggests that a hot plume source rose in the Permian.

Bornholm and the evolution of the Baltic shield

The Kelseaa dyke was intruded about 100 Ma after a major rejuvenation of the Gothic crust at 1.45 Ga according to the extensive data base for the gneiss and granites of Bornholm (Tschernoster, 2000; Čečys, 2004; Obst et al., 2004, Zariņš & Johansson, 2008). It therefore seems most likely that this major dyke marks a NE-trending rifting event of Baltica at around 1326 Ma. The N- to NE-trending Kungsbacka bimodal suite (1.34-1.30 Ga) south of Lake Vänern and west of the Protogine Zone and related dolerite with an age of just under 1.30 Ga have recently been suggested to be emplaced during a continental rifting event (Austin Hegardt et al., 2007; Söderlund et al., 2008). Although these occurrences are > 200 km apart, they are the only reported events at the time of the Kelseaa intrusion. In the case of the Kelseaa magma, rifting most likely developed in a back-arc setting.

The events forming the CSDG took place in the interval 1270-1250 Ma and have been explained as being related to extension behind an active margin with subduction along the Laurentia-Baltica continental margin preceding Rodinia formation (Söderlund et al., 2006). Solyum et al. (1992) considered that the CSDG was intracratonic and unrelated to continental rifting. However, the CSDG seems to be somewhat earlier than the type 2 dykes (c. 1220 Ma) of Bornholm.

Datings of zircon and baddeleyite from ultramafic, mafic and felsic intrusions including N-S trending dolerites in the Protogine zone define two distinct magmatic events at c. 1204 and c. 1220 Ma (Söderlund et al., 2004; Söderlund et al., 2005, Söderlund & Ask, 2006), significantly older than the c. 1180 Ma previously suggested by Johansson & Johansson (1990). These events then seem contemporaneous with the type 2 Bornholm dykes. The Protogine Zone magmatic events were thought to be related to back-arc spreading during the closure of an ocean from 1.25 Ga until 1.13 Ga at the beginning of the Sveconorwegian orogeny (Söderlund & Ask, 2006). The new precise age information for the Protogine Zone magmatism separates this from both the Gardar and the MacKenzie events (LeCheminant & Heaman, 1989; Upton et al., 2003). However, the composition of the Protogine Zone Dolerite Group (PZDG) (Solyum et al., 1992) is very different from the type 2 dykes of Bornholm, for which we suggest a mantle plume origin, and they were probably not related.

The Blekinge Dalarne Dolerite Group (BDDG) was intruded at 978-945 Ma based on U-Pb and Lu-Hf on baddeleyite and zircon (Söderlund et al., 2004, Söderlund et al., 2005). This is somewhat earlier than the c. 930 Ma based on Sm-Nd whole rock isochrons (Johansson & Johansson, 1990) which are in accordance with most of Rb-Sr age determinations of Patchett (1978). These dykes occur in a zone parallel to the Protogine Zone and extend for 700 km from Dalarne in the north to the south coast of Blekinge where they trend approximately N-S just north of Bornholm (Fig. 1). The Sveconorwegian and Grenvillian orogenies took place in the period 1.13 – 0.95 Ga (Andréasson & Rohde, 1990) with peak metamorphism at 972 Ma (Johansson et al., 2001). Solyum et al. (1992) considered that the BDDG were emplaced as part of the earliest phase of a late Proterozoic rifting of Baltica which encompassed graben formation in the Protogine Zone (Andréasson & Rodhe, 1990). Söderlund & Ask (2006) described the intrusion of the BDDG as contemporaneous with exhumation of the high-grade rocks of the orogeny and taking place in the Sveconorwegian foreland, and suggested that the graben formation at lake Vättern in the Protogine Zone was an analogue to the Permian Oslo rift. The Kaas and Listed dykes are quite similar to some BDDG dykes and may be part of these events.

The NW-trending Permian dykes, including the trachytic Bjergebakke dyke, have been correlated with the Scania dykes of similar age (Obst et al. 2000), and are thus related to the Oslo rift and other rifts in the Skagerrak and the North Sea, and in general to the breakup of Pangea.

Conclusions

The more than 250 dykes on Bornholm represent significant events of mafic magmatism related to rifting at the edge of the Baltic craton in the mid to late Proterozoic and Permian. The dykes occur in all basement rocks, although more rarely in the granites than in the gneisses. In four dyke swarms basaltic materials constitute 10 - 20 % of the crust. The dykes comprise four distinct types based on age information, mode of occurrence, petrography and geochemistry:

1) The Kelseaa dyke and Kelseaa-like dykes at 1326 Ma are NE-trending olivine tholeiites comprising the 60 m Kelseaa gabbroic-doleritic dyke and two others.

The Kelseaa magmas were derived from depleted mantle enriched in fluid-mobile elements and contaminated in the crust, probably in a back-arc setting. One Kelseaa-like dyke has N-MORB character.

2) More than 200 narrow NNW- to NNE-trending dykes probably intruded around 1220 Ma. Most of them are alkali basalts-trachybasalts-basanites with potassic character. A few differentiates range to phonotephritic compositions. One subtype of basanitic or potassic trachybasaltic composition is particularly enriched in incompatible elements.

The magmas of the narrow dykes may be related by fractionation of olivine, followed by olivine + clinopyroxene to a few more evolved dykes. They were mainly derived from a mantle plume. The plume source of recycled oceanic crust consisted of typical OIB-type peridotite and probably a garnet pyroxenite of gabbroic origin. A more enriched subgroup was derived at greater depths by a few percent melting of peridotite, probably at higher temperatures. The narrow dykes may be contemporaneous with the Protogine Zone Dolerite Group of southern Sweden, but have a different origin.

3) The large dykes at Listed and Kaas, and some Kaas-like smaller dykes, comprise a group of evolved transitional rocks (shoshonites and mugearites) intruded around 950 Ma.

The source of the Kaas-Listed dykes was rather depleted, probably sublithospheric mantle. Geochemically they resemble the c. 950 Ma Blekinge Dalarne Dolerite Group and may be closely related to these.

4) A few WNW- and NW-trending dykes are Permian (c. 300 Ma old) quartz tholeiites.

The magmas injected in the NW-trending dykes were derived at rather shallow depths by relatively high degrees of melting of most likely a hot mantle plume. The source displays a distinct OIB-type geochemistry different from the narrow dyke sources, and was more enriched than sources for other Bornholm dyke magmas.

Acknowledgements

We thank John Bailey for trace element XRF analyses and Raymond Gwozdz for INA analyses. We are grateful for the help from Trine Dirks with collection of some of the samples and for company in the field of B. and H. Viuf and B. and H. Jensen. Niels Abrahamsen and Asger Ken Pedersen contributed with contructive reviews that improved the paper, and the comments and editorial handling of J. Richard Wilson are greatly acknowledged.

Dansk sammendrag

Bornholms mafiske gange repræsenterer mellem proterozoiske til permiske magmatiske hændelser i randen af Det Baltiske Kraton. Flere hundrede gange er intruderede i det prækambriske grundfjelds gnejser og graniter. Feltforhold og 60 nye kemiske analyser af hoved- og sporgrundstoffer præsenteres. Gruppering baseret på evidens fra felten, geokemi og petrologi indikerer at gangintrusionerne kan korreleres med begivenheder for henholdsvis 1326 Ma (Kelseaa gangen), 1220 Ma (de smalle gange), 950 Ma (Kaas-Listed gangene) og 300 Ma (NW- eller WNW-strygende gange) siden. Den største gang ved Kelseaa (60 m bred) og nogle relaterede gange er primitive olivin tholeiiter af hvilke en har N-MORB (normaltype midtoceanrygsbasalt) geokemiske træk; alle er skorpekontaminerede. Kelseaa-type magmaer blev dannet i ret ringe dybde fra en fluid-beriget relativt forarmet kappekilde, men nogle har en komponent, som er dannet fra en kappekilde med residual granat. Deres dannelse foreslås at være i et backarc-miljø.

De mere end 200 smalle gange er olivin tholeiiter (hvoraf nogle er pikritiske), alkali basalter, trachybasalter og basaniter (hvoraf nogle er pikritiske), og omfatter kun få udviklede phonotephriter. Magmaerne udvikledes ved olivin og olivin + clinopyroxenfraktionering. De har sporgrundstof geokemiske karaktertræk, som kan beskrives hovedsaglig ved to komponenter, af hvilke en er et typisk OIB-magma (OIB = oceanøbasalt) (La/Nb < 1, Zr/Nb = 4, Sr/Nd = 16) og afledt fra spinel peridotit i et temmelig højt kappeniveau, hvorimod den anden er beriget på Sr, har La/Nb = 1.0-1.5, Zr/Nb = 9, Sr/Nd = 30, og var afledt fra større dybde fra en oprindeligt gabbroisk kilde. Begge kilder var sandsynligvis recirkuleret materiale i en kappediapir. Et mindre antal af disse gange er meget mere beriget i inkompatible grundstoffer og blev dannet fra granatperidotit ved en lav grad af opsmeltning. De få andre store gange (20-40 m) og relaterede gange er alle udviklede trachybasalter og basaltiske trachyandesiter. De synes at være relaterede til Blekinge-Dalarne doleritgruppen. De få NW-gående gange er kvarts tholeiiter, som blev dannet ved en høj grad af opsmeltning under relativt lavt tryk af en mere beriget kappe end andre bornholmske gange. Dette implicerer at kappen formentlig var en meget varm diapir.

References

Åberg, G. 1988: Middle Proterozoic anorogenic magmatism in Sweden and worldwide. Lithos 21, 279-289.

Abrahamsen, N. 1977: Palaeomagnetism of 4 dolerite dykes around Listed, Bornholm Denmark . Bulletin of the Geological Society of Denmark 26, 245-264.

Abrahamsen, N. & Lewandowski, M. 1995: Palaeomagnetism of Proterozoic dykes from Bornholm, Denmark. Geophysical Journal International 121, 949-962.

Anders, E. & Grevesse, N. 1989 Abundances of the elements: Meteoritic and solar. Geochmica Cosmochimica Acta 53, 197-214.

Andréasson, P.-G. & Rodhe, A. 1990: Geology of the Protogine Zone south of lake Vättern, Southern Sweden: a reinterpretation. Geologiska Föreningens i Stockholm förhandlingar 112, 107-126.

Austin Hegardt, E., Cornell, D.H., Hellström F.A. & Lundqvist, I. 2007: Emplacement ages of the mid-Proterozoic Kungsbacka Bimodal Suite, SW Sweden. Geologiska Föreningens i Stockholm förhandlingar 129, 227-234.

Berthelsen, A. 1989: Bornholms grundfjeld. Varv 1989,1, 3-39.

Berthelsen, A. 1992: Mobile Europe. In: D. Blundell, R. Freeman & S. Mueller (Editors), A Continent Revealed: The European Geotraverse. Cambridge University Press, Cambridge, pp. 11-32.

Bogdanova, S.V. 2001: Tectonic settings of 1.65-1.4 Ga AMCG magmatism in the western East European Craton, western Baltica. Journal of Conference Abstracts 6, 769.

Bogdanova, S.V., Bingen, B., Gorbatschev, R., Kheraskova, T.N., Kozlov, V.I., Puchkov, V.N. & Volozh, Y.A. 2008: The East European Craton Baltica before and during the assembly of Rodinia. Precambrian Research 160, 23-45.

Bruun-Petersen, J. 1975: Origin and correlation of the sandstone dykes at Listed, Bornholm Denmark. Bulletin of the Geological Society of Denmark 24, 33-44.

Callisen, K. 1934: Das Grundgebirge von Bornholm. Danmarks Geologiske Undersøgelse, II. række 50, 266 pp.

Čečys, A. 2004: Tectonic implications of the ca. 1.45 Ga granitoid magmatism at the southwestern margin of the East European Craton. Unpublished Ph. D. thesis, University of Lund, Sweden, 115 pp.

Čečys, A. & Benn, K. 2007: Emplacement and deformation of the c. 1.45 Ga Karlshamn granitoid pluton, southeastern Sweden, during ENE-WSW Danopolonian shortening. International Journal of Earth Sciences 96, 397-414.

Chauvel, C. & Hémond, C. 2000: Melting of a complete section of recycled oceanic crust: trace element and Pb isotopic evidence from Iceland. Geochemistry, Geophysics, Geosystems 1, 1999GC000002.

Clague, D.A. & Frey, F.A. 1982: Petrology and Trace Element Geochemistry of the Honolulu Volcanics, Oahu: Implications for the Oceanic Mantle below Hawaii. Journal of Petrology 23, 447-504.

Dupuy, C., Barsczus, H.G., Liotard, J.-M. & Dostal, J. 1988: Trace element evidence for the origin of ocean island basalts: An example from the Austral Islands. Contributions to Mineralogy and Petrology 98, 293-302.

Eisele, J., Sharma, M., Galer, S.J.G., Blichert-Toft, J., Devey, C.W. & Hofmann, A.W. 2002: The role of sediment recycling in EM-1 inferred from Os, Pb, Hf, Nd, Sr isotope and trace element systematics of the Pitcairn hotspot. Earth and Planetary Science Letters 196, 197-212.

Forchhammer, G. 1847: Gebirgsbildung des Königsreichs Dänemarks. Copenhagen.

Gorbatschev, R., Solyom, Z. & Johansson, I. 1979: The Central Scandinavian Dolerite Group in Jämtland, central Sweden. Geologiska Föreningens i Stockholm förhandlingar 101, 3, 177-190.

Hofmann, A.W. 1988: Chemical differentiation of the Earth: the relationship between mantle, continental crust, and oceanic crust. Earth and Planetary Science Letters 90, 297-314.

Hofmann, A.W. 1997: Mantle geochemistry: the message from oceanic volcanism. Nature 385, 219-229.

Holm, P.M., Heaman, L.M. & Pedersen, L.E. 2005: First direct age determination for the Kelseaa Dolerite Dyke, Bornholm, Denmark. Bulletin of the Geological Society of Denmark 52, 1-6.

Holm, P.M., Wilson, J.R., Christensen, B.P., Hansen, L., Hansen, S.L., Hein, K.M., Mortensen, A.K., Pedersen, R., Plesner, S. & Runge, M. 2006: Sampling the Cape Verde Mantle Plume: Evolution of Melt Compositions on Santo Antão, Cape Verde Islands. Journal of Petrology 47, 145-189.

Jensen, A. 1966: Mineralogical variations across two dolerite dykes from Bornholm. Meddelelser fra dansk geologisk Forening 16, 370-455.

Jensen, A. 1988: The Bjergebakke dyke - a kullaite from Bornholm. Bulletin of the Geological Society of Denmark 37, 123-140.

Johansson, L. & Johansson, Å. 1990: Isotope geochemistry and age relationships of mafic intrusions along the Protogine Zone, southern Sweden. Precambrian Research 48, 395-414.

Johansson, L., Möller, C. & Söderlund, U. 2001: Geochronology of eclogite facies metamorphism in the Sveconorwegian Province of SW Sweden. Precambrian Research 106, 261-275.

Johansson, Å. & Larsen, O. 1989: Radiometric age determinations and Precambrian geochronology of Blekinge, southern Sweden. Geologiska Föreningens i Stockholm förhandlingar 111, 1, 35-50.

Johansson, Å., Bogdanova, S. & Čečys, A. 2006: A revised geochronology for the Blekinge Province, southern Sweden. Geologiska Föreningens i Stockholm förhandlingar 128, 287-302.

Klein, E.M., & Langmuir, C.M. 1987: Global correlation of ocean ridge basalt chemistry with axial depth and crustal thickness. Journal of Geophysical Research 92, 8090-8115.

Klingspor, I. 1976: Radiometric age-determination of basalts, dolerites and related syenite in Skåne, southern Sweden. Geologiska Föreningens i Stockholm förhandlinger 98, 195-216.

Kokfelt, T.F., Hoernle, K., Hauff, F., Fiebig, J., Werner, R. & Garbe-Schönberg, D. 2006: Combined Trace Element and Pb-Nd-Sr-O Isotope Evidence for Recycled Oceanic Crust (Upper and Lower) in the Iceland Mantle Plume. Journal of Petrology 47, 9, 1705-1749.

Larsen, O. 1980: Geologisk aldersbestemmelse ved isotopmålinger. Dansk Natur - Dansk Skole, årsskrift for 1980, 89-106.

Le Bas, M.J. 2000: Reclassification of the high-Mg and picritic volcanic rocks. Journal of Petrology 41, 1467-1470.

LeCheminant, A.N. & Heaman, L.M. 1989: MacKenzie igneous events, Canada: middle Proterozoic hotspot magmatism associated with ocean opening. Earth and Planetary Science Letters 96, 38-48.

Le Maitre, R. W. 1989: A Classification of Igneous Rocks and Glossary of Terms. Blackwell Scientific Publications, Oxford, 193 pp.

Lewandowski, M. & Abrahamsen, N. 2003: Paleomagnetic results from the Cambrian and Ordovician sediments of Bornholm (Denmark) and Southern Sweden and paleogeographical implications for Baltica. Journal of Geophysical Research 108, 2516, doi: 10.1029/2002JB002281.

McDonough, W.F. & Sun, S.-s. 1995: The composition of the Earth. Chemical Geology 120, 223-253.

McKenzie, D., & O'Nions, R.K. 1991: Partial Melt Distribution from Inversion of Rare Earth Element Concentrations. Joural of Petrology 32, 1021-1091.

Micheelsen, H.I, 1961. Bornholms grundfjæld. Meddelelser fra dansk geologisk Forening 14, 308-347.

Middlemost, E.A.K. 1989: Iron oxidation ratios, norms and the classification of volcanic rocks. Chemical Geology 77, 19-26.

Münther, V. 1945a: Diabasgangene paa Bornholm: En undersøgelse af de vigtigste bornholmske Sprækkedale og en redegørelse for Diabasens Relation til Granitens Forkløftning, 217pp. Unpublished prize paper. University of Copenhagen, Copenhagen.

Münther, V. 1945b: Sprækkedale og diabasintrusioner på Bornholm. Meddelelser fra dansk geologisk Forening 10, 641-645.

Münther, V. 1973. Dominerende forkastninger på Bornholm. Danmarks Geologiske Undersøgelse, II. række 85, 161 pp.

Obst, K. 2000: Permo-Carboniferous dyke magmatism on the Danish island Bornholm. Neues Jahrbuch der Geologie und Paläontologie Abhandlungen 218, 243-266.

Obst, K., Hammer, J., Katzung, J. & Korich, D. 2004: The Mesoproterozoic basement in the southern Baltic Sea: insights from the G 14-1 off-shore borehole. International Journal of Earth Sciences 93, 1-12.

Palacz, Z. & Saunders, A.D. 1986: Coupled trace element and isotope enrichment in the Cook-Austral-Samoa islands, southwest Pacific. Earth and Planetary Science Letters 79, 270-280.

Patchett, P. J. 1978: Rb/Sr ages of Precambrian dolerites and syenites in southern and central Sweden. Sveriges Geologiska Undersökning, ser. C 747, 63pp.

Patchett, P.J., Lehnert, K., Rehkämper, M. & Sieber, G. 1994: Mantle and crustal effects on the geochemistry of Proterozoic dikes and sills in Sweden. Journal of Petrology 35: 1095-1125.

Platou, S.W. 1970: The Svaneke granite complex. Bulletin of the Geological Society of Denmark 20, 93-133.

Rudnick, R.L. & Gao, S. 2003: Composition of the Continental Crust. In: Turekian, K.K. & Holland, H.D. (Editors.) Treatise of Geochemistry. Elsevier, Chapter 3.01, 64pp.

Saxov, S. 1958: Keldseå Diabas Dike and Gravity, Geodætisk Institut Meddelelse No. 35.

Söderlund, U. & Ask, R. 2006: Mesoproterozoic bimodal magmatism along the Protogine Zone, S Sweden: three magmatic pulses at 1.56, 1.22 and 1.205 Ga, and regional implications. Geologiska Föreningens i Stockholm förhandlingar 128, 303-310.

Söderlund, U., Patchett, P. J., Vervoort, J. D. & Isachsen, C. E. 2004: The decay constant of ^{176}Lu determined from Lu-Hf and U-Pb isotope systematics of terrestrial Precambrian high-temperature mafic intrusions. Earth and Platetary Science Letters 219, 311-324

Söderlund, U., Isachsen, C.E., Bylund, G., Heaman L.M., Patchett, P.J., Vervoort, J.D. & Andersson U.B. 2005: U-Pb baddeleyite ages and Hf, Nd isotope chemistry constraining repeated mafic magmatism in the Fennoscandian Shield from 1.6 to 0.9 Ga. Contributions to Mineralogy and Petrology 150, 174-194.

Söderlund, U., Elming, S.-Å., Ernst, R.E. & Schissel, D. 2006: The Central Scandinavian Dolerite Group – Protracted hotspot activity or back-arc magmatism? Constraints from U-Pb baddeleyite geochronology and Hf isotopic data. Precambrian Research 150, 136-152.

Söderlund, U., Hellström F.A. & Kamo S.L. 2008: Geochronology of high-pressure mafic granulite dykes in SW Sweden: tracking the P-T-t path of metamorphism using Hf isotopes in zircon and baddeleyite. Journal of Metamorphic Geology 26, 539-560.

Solyom, Z., Lindqvist, J.-E. & Johansson, I. 1992: The geochemistry, genesis, and tectonic setting of Proterozoic mafic dyke swarms in southern and central Sweden. Geologiska Föreningens i Stockholm förhandlingar 114, 47-65.

Stracke, A. & Bourdon, B. 2009: The importance of melt extraction for tracing mantle heterogeneity. Geochimica Cosmochimica Acta 73, 218-238.

Sun, S.-s. & McDonough, W.F. 1989: Chemical and isotopic systematics of oceanic basalts: implications for mantle composition and processes. In: A.D. Saunders & M.J. Norry (Editors) Magmatism in the ocean basins. Geological Society of London Special Publication 42, 313-345.

Surlyk, F. 1980: Denmark. In: Geology of the European Countries, Proceedings of the 26th International Geological Congress, Paris. Graham & Trotman Ltd, Bordas, pp.1-50.

Tschernoster, R. 2000: Isotopengeochemische Untersuchungen am Detritus der Dänisch-Norddeutsch-Polnischen Kaledoniden und deren Vorland. Unpublished Ph.D. thesis, Rheinisch-Westfälischen Technischen Hochschule, Aachen, 128 pp.

Tainton, K.M. & McKenzie, D. 1994: The generation of kimberlites, lamproites, and their source rocks. Journal of Petrology 35, 787-817.

Ulmer, P. 1989: Partitioning of high field strength elements among olivine, pyroxenes, garnet and calc-alkaline picrobasalt: experimental results and an application. Annual Report of the Director of the Geophysical Laboratory 1988/1989: 42-47.

Upton, B.G.J., Emeleus, C.H., Heaman, L.M., Goodenough, K.M. & Finch, A.A. 2003: Magmatism of the mid-Proterozoic Gardar Province, South Greenland: chronology, petrogenesis and geological setting. Lithos 68, 43-65.

Weaver, B.L. 1991: The origin of ocean island basalt end-mem-

ber compositions: trace element and isotopic constraints. Earth and Planetary Science Letters 104, 381-397.
Weaver, B.L., Wood, D.A., Tarney, J. & Joron, J.-L. 1987: Geochemistry of ocean island basalts from the South Atlantic: Ascension, Bouvet, St. Helena, Gough and Tristan da Cunha. In: J.G. Fitton & B.G.J. Upton (Editors), Alkaline Igneous Rocks. Geological Society of London Special Publication 30, 253-267.
Woodhead, J.D. 1996: Extreme HIMU in an oceanic setting: the geochemistry of Mangaia Island (Polynesia), and temporal evolution of the Cook-Austral hotspot. Journal of Volcanology and Geochermal Research 72, 1-19.
Zariņš, K. & Johansson Å. 2008: U-Pb geochronology of gneisses and granitoids from the Danish island of Bornholm: new evidence for 1.47-1.45 Ga magmatism at the southwestern margin of the East European Craton. International Journal of Earth Sciences. doi 10.1007/s0531-008-0333-0.
Zindler, A. & Hart, S.R. 1986: Chemical geodynamics. Annual Reviews in Earth and Planetary Sciences 14, 493-571.

Appendix

Comparison between measured and reference values for some standards, internal analytical precision and detection limits for XRF, INAA and ICP-MS trace element analyses.

	XRF				INAA					ICP-MS							
	Prec-ision	LLD$	Standard		Prec-ision	LLD$	Standard			LLD$	Blank	Standards					
			AGV-1	AGV-1			BHVO1					DNC-1	DNC-1	W-2a	W-2a	BIR-1a	BIR-1a
Element	rel% (1•)	meas@ ppm	meas@ ppm	Ref.* ppm	rel% (1•)	meas@ ppm	meas@ ppm AVG	1•• ppm N=5	Ref.* ppm	meas@ ppm	meas@ ppm	meas@ ppm	Ref.* ppm	meas@ ppm	Ref.* ppm	meas@ ppm	Ref.* ppm
Sc	5	<1	13	12.1	0.2	0.006	31.7	0.5	31.8	1		31	31	36	36	43	44
V	5	<3	119	123						5		156	148	281	262	336	313
Cr	5	<3	11	12						20	< 20	290	285	90	92	380	382
Co	4	<1	12.5	15						1	< 10	56	54.7	43	43	50	51.4
Ni	2	<1	14	17						20	< 30	260	247	60	70	150	166
Cu	5	<2	58	60						10	< 1	100	96	110	110	120	126
Zn	5	<1	84	88						30	< 0.5	120	66	130	80	100	71
Ga	5	<1	20	20						1	< 5	14	15	17	17	14	16
Rb	2	<0.5	66	67						2	< 1	4	4.5	20	21	< 2	0.25
Sr	1	<0.5	652	662						2		142	145	195	190	108	108
Y	5	<1	20	21						2	< 20	13	18	17	24	11	16
Zr	2	<1	223	225						4	< 1	47	41	98	94	23	16
Nb	2	<0.5	14.4	15						1	< 0.2	1	3	7	7.9	< 1	0.6
Ba	2	<1	1204	1221	8	26	139	16		3		102	114	168	182	7	7
La	2	<1	38	38	0.7	0.07	16.3	0.4	13.8	0.1	< 0.05	3.6	3.8	10.2	10	0.7	0.62
Ce	2	<2	69	66	0.4	0.45	39	3	39	0.1	< 0.05	8	10.6	22.5	23	2	1.95
Nd	4	<1	34	34	10	5	27.1	1.9	25.2	0.1	< 0.05	4.7	4.9	12.1	13	2.2	2.5
Sm					0.6	0.05	6.2	0.4	6.2	0.1	< 0.01	1.4	1.38	3.1	3.3	1	1.1
Eu					0.6	0.009	2.07	0.03	2.06	0.05	< 0.005	0.59	0.59	1.08	1	0.52	0.54
Tb					8	0.07	1.03	0.1	0.96	0.1	< 0.01	0.4	0.41	0.7	0.63	0.4	0.36
Yb					5	0.1	1.6	0.2	2.02	0.1	< 0.01	2	2.01	2	2.1	1.6	1.65
Lu					5	0.02	0.27	0.05	0.291	0.04	< 0.002	0.3	0.32	0.3	0.33	0.25	0.26
Hf					0.6	0.05	4.4	0.2	4.38	0.2	< 0.1	1.1	1.01	2.6	2.6	0.7	0.6
Ta					1	0.03	1.17	0.08	1.23	0.1	< 0.01	0.1	0.098	0.5	0.5	< 0.1	0.04

*) Govindaraju, k. (1994) Geostandards Newsletter 18, Special Issue, 1-158. $) LLD = Lower Limit of Detection. @) Measured value